

Preservation of the Global Knowledge by Not-True Self Knowledge Distillation in Federated Learning

Gihun Lee*, Minchan Jeong*, Yongjin Shin, Sangmin Bae, Se-Young Yun
KAIST

{opcrisis, mcjeong, yj.shin, bsmn0223, yunseyoung}@kaist.ac.kr

Abstract

In federated learning, a strong global model is collaboratively learned by aggregating clients' locally trained models. Although this precludes the need to access clients' data directly, the global model's convergence often suffers from data heterogeneity. This study starts from an analogy to continual learning and suggests that *forgetting* could be the bottleneck of federated learning. We observe that the global model forgets the knowledge from previous rounds, and the local training induces forgetting the knowledge outside of the local distribution. Based on our findings, we hypothesize that tackling down forgetting will relieve the data heterogeneity problem. To this end, we propose a novel and effective algorithm, *Federated Not-True Distillation* (FedNTD), which preserves the global perspective on locally available data only for the *not-true* classes. In the experiments, FedNTD shows state-of-the-art performance on various setups without compromising data privacy or incurring additional communication costs.

1 Introduction

At present, massive data is being collected from edge devices such as mobile phones, vehicles and facilities. As the data may be distributed on numerous devices, decentralized training is often required to train deep network models. Federated learning [25, 26] is a distributed learning paradigm that enables the learning of a global model while preserving clients' data privacy. In federated learning, clients independently train local models using their private data, and the server aggregates them into a single global model. In this process, most of the computation is performed by client devices, while the global server only aggregates the model parameters and distributes them to clients [2, 52].

Most federated learning algorithms are based on FedAvg [39], which aggregates the locally trained model parameters by weighted averaging proportional to the amount of local data that each client had. While various federated learning algorithms have been proposed thus far, they each conduct parameter averaging in a certain manner [1, 9, 21, 32, 50, 53]. Although this aggregation scheme empirically works well and provides a conceptually ideal framework when all client devices are active and i.i.d. distributed (a.k.a. LocalSGD), the data heterogeneity problem [33, 56] is a notorious challenge for federated learning applications and prevents their widespread applicability [20, 31].

As the client generates its own data, the data is not identically distributed. More precisely, the local data across clients are drawn from heterogeneous underlying distributions; thereby, locally available data fail to represent the overall global distribution, which is referred to as data heterogeneity. Despite its inevitable occurrence in many real-world scenarios, data heterogeneity not only makes theoretical analysis difficult [33, 56] also degrades many federated learning algorithms' performances [18, 29]. By resolving the data heterogeneity problem, learning becomes more robust against partial participation [33, 39], and the communication cost is also reduced by faster convergence [49, 53].

Interestingly, continual learning [43, 48] faces a similar challenge. In continual learning, a learner model is continuously updated on a sequence of tasks, with an objective to perform well on whole

* Equal contribution.

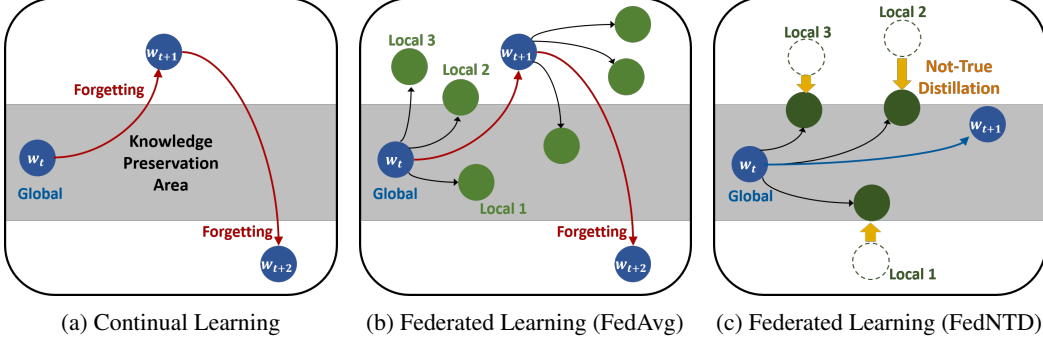


Figure 1: An overview of forgetting in learning scenarios. As catastrophic forgetting in (a) Continual Learning, (b) Federated Learning also experiences forgetting. However, (c) FedNTD prevents forgetting by preserving global knowledge during local training.

tasks. Unfortunately, owing to the heterogeneous data distribution of each task, learning on the task sequence often results in *catastrophic forgetting* [38, 41], whereby fitting on a new task interferes with the important parameters for previous tasks. As a consequence, the model parameters drift away from the area where the previous knowledge is desirably preserved (Figure 1a).

Our first conjecture is such forgetting also exists in federated learning. While the server aggregates local models, the distribution where they are trained may be largely different from those of previous rounds. As a result, the global model faces the distributional shifts at each round, which may cause the forgetting as in continual learning (Figure 1b). To empirically verify this analogy, we examine the global model’s prediction consistency. More specifically, we measure the global model’s class-wise accuracy while the communication rounds proceed.

The observations verify our conjecture: the global model’s prediction is highly inconsistent across communication rounds, significantly reducing the performance of predicting some classes that the previous model originally predicted well. We dig deeper to analyze how averaging the locally updated parameters induces such forgetting and confirm that it occurs in local training: the global knowledge, corresponding to the outside of local distribution, is prone to be forgotten. As merely averaging the local models cannot recover it, the global model struggles to preserve previous knowledge.

Based on our findings, we hypothesize that mitigating the issue of forgetting can relieve data heterogeneity (Figure 1c). To this end, we propose a novel algorithm Federated Not-True Distillation (FedNTD). FedNTD utilizes the global model’s prediction on locally available data, but only for the not-true classes. We demonstrate the effect of FedNTD on preserving global knowledge outside of a local distribution and its benefits on federated learning. Experimental results show that FedNTD achieves state-of-the-art performance in various setups.

To summarize, our contributions are:

- We present a systematic study on forgetting in federated learning. The global knowledge outside of the local distribution is prone to be forgotten and is closely related to the data heterogeneity issue (Section 2).
- We propose a simple yet effective algorithm, FedNTD, to prevent forgetting. Unlike prior works, FedNTD neither compromises data privacy nor incurs additional communication burden. We validate the efficacy of FedNTD on various setups and show consistently achieves state-of-the-art performance (Section 3, Section 4).
- We analyze the FedNTD benefits on the federated learning. The knowledge preservation by FedNTD improves weight alignment and weight divergence after local training (Section 5).

1.1 Preliminaries

Federated Learning We aim to train an image classification model in federated learning system that consists of K clients and a central server. Each client k has a local dataset \mathcal{D}^k , where the whole dataset $\mathcal{D} = \bigcup_{k \in [K]} \mathcal{D}^k$. At each communication round t , the server distributes the current global model parameters $w^{(t-1)}$ to sampled local clients $K^{(t)}$. Starting from $w^{(t-1)}$, each client $k \in K^{(t)}$ updates the model parameters $w_k^{(t)}$ using its local datasets \mathcal{D}^k with the following objective:

$$w_k^{(t)} = \underset{w}{\operatorname{argmin}} \mathbb{E}_{(x,y) \sim \mathcal{D}^k} [\mathcal{L}(w; w^{(t-1)}, x, y)]. \quad (1)$$

where \mathcal{L} is the loss function. At the end of round t , the sampled clients upload the locally updated parameters back to the server and aggregate by parameter averaging as $w^{(t)}$ as follows:

$$w^{(t)} = \sum_{k \in K^{(t)}} \frac{|\mathcal{D}^k|}{\sum_{k' \in K^{(t)}} |\mathcal{D}^{k'}|} w_k^{(t)}. \quad (2)$$

Knowledge Distillation Given a teacher model T and a student model S , knowledge distillation [17] matches their softened probability q_τ^T and q_τ^S using temperature τ . The c -th value of the q_τ can be described as $q_\tau(c) = \frac{\exp(z_c/\tau)}{\sum_i \exp(z_i/\tau)}$, where z_c is the c -th value of logits vector z and \mathcal{C} is the number of classes. Given a sample x , the student model S is learned by a linear combination of cross-entropy loss \mathcal{L}_{CE} for one-hot label $\mathbb{1}_y$ and Kullback-Leibler divergence loss \mathcal{L}_{KL} using a hyperparameter β :

$$\mathcal{L} = (1 - \beta)\mathcal{L}_{CE}(q, \mathbb{1}_y) + \beta\tau^2\mathcal{L}_{KL}(q_\tau^S, q_\tau^T) \quad (3)$$

$$\mathcal{L}_{CE}(q, \mathbb{1}_y) = -\sum_{c=1}^C \mathbb{1}_y(c) \log q(c), \quad \mathcal{L}_{KL}(q_\tau^S, q_\tau^T) = -\sum_{c=1}^C q_\tau^T(c) \log \left[\frac{q_\tau^S(c)}{q_\tau^T(c)} \right] \quad (4)$$

2 Forgetting in Federated Learning

To understand how the non-IID data affects federated learning, we perform an experimental study on heterogeneous locals. We choose CIFAR-10 [27] and a convolutional neural network with four layers as in [39]. We split the data to 100 clients using Latent Dirichlet Allocation (LDA), assigning the partition of class c samples to clients by $p \sim \text{Dir}(\alpha)$. The heterogeneity level increases as the α decreases. We train the model with FedAvg for 200 communication rounds, and 10 randomly sampled clients are optimized for 5 local epochs at each round. More details are in [Appendix C](#).

2.1 Global Model Prediction Consistency

To confirm our conjecture on forgetting, we first consider how the global model’s prediction varies as the communication rounds proceed. If the data heterogeneity induces forgetting, the prediction after update (i.e., parameter averaging) may be less consistent compared to the previous round. To examine it, we observe the model’s class-wise test accuracy at each round, and measure its similarity to the previous round. The results are provided in [Figure 2a](#) and [Figure 2b](#).

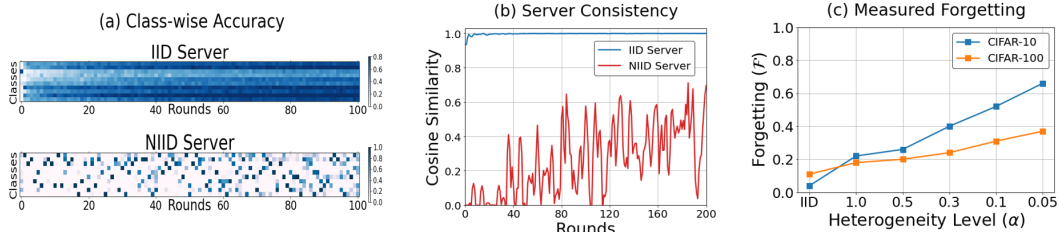


Figure 2: Forgetting analysis on the global server model. (a): Class-wise test accuracy on CIFAR-10 IID and NIID ($\alpha=0.1$) cases. (b): Cosine similarity of class-wise accuracy vector w.r.t. previous round global model on IID and NIID ($\alpha = 0.1$) cases. (c): Forgetting \mathcal{F} by different heterogeneity levels on CIFAR-10 and CIFAR-100.

As expected, while the server model learned from i.i.d. locals (IID Server) predicts each class evenly well at each round, prediction is highly inconsistent in the non-IID case (NIID Server). In the non-IID case, the test accuracy on some classes which originally predicted well by the previous global model often drops significantly. This implies that forgetting occurs in federated learning.

To measure how the forgetting is related to data heterogeneity, we borrow the idea of *Backward Transfer* (BwT) [5], a prevalent forgetting measure in continual learning [4, 7, 8, 13], as follows:

$$\mathcal{F} = \frac{1}{\mathcal{C}} \sum_{c=1}^C \max_{t \in \{1, \dots, T-1\}} (\mathcal{A}_c^{(t)} - \mathcal{A}_c^{(T)}) \quad (5)$$

where $\mathcal{A}_c^{(t)}$ is the accuracy on class c at round t . Note that the forgetting measure \mathcal{F} captures the averaged gap between peak accuracy and the final accuracy for each class at the end of learning. The result on the varying heterogeneity levels is plotted in [Figure 2c](#), showing that the global model suffers from forgetting more severely as the heterogeneity level increases.

2.2 Knowledge Outside of Local Distribution

We take a closer look at local training to investigate why aggregating the local models induces forgetting. In the continual learning view, a straightforward approach is to observe how fitting on the new distribution degrades the performance of the old distribution. However, in our problem setting, the local clients can have any class. Given that only their portions in the local distribution differ across clients, such strict comparison is intractable. Hence, we formulate *in-local distribution* $p(\mathcal{D})$ and its *out-local distribution* $\tilde{p}(\mathcal{D})$ to systematically analyze forgetting in local training.

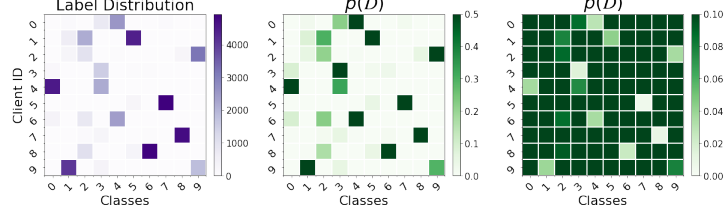


Figure 3: An example of in-local distribution $p(\mathcal{D})$ and out-local distribution $\tilde{p}(\mathcal{D})$ on CIFAR-10 ($\alpha = 0.1$).

Definition 1. Consider a local dataset \mathcal{D} consists of N data points x_i and its label y_i in C -class classification problem. The **in-local distribution vector** $p^k = p(\mathcal{D}^k)$ and its **out-local distribution vector** $\tilde{p}^k = \tilde{p}(\mathcal{D}^k)$ are

$$p = [p_1, \dots, p_C], \quad \text{where } p_c := \frac{1}{N} \sum_{i=1}^N \mathbb{I}(y_i = c) \quad (6)$$

$$\tilde{p} = [\tilde{p}_1, \dots, \tilde{p}_C], \quad \text{where } \tilde{p}_c := \frac{1}{C-1} (1 - p_c) \quad (7)$$

The underlying idea of out-local distribution $\tilde{p}(\mathcal{D})$ is to assign a higher proportion to the classes with fewer samples in local datasets. Accordingly, it corresponds to the region in the global distribution where the in-local distribution $p(\mathcal{D})$ cannot represent. Note that if $p(\mathcal{D})$ is uniform, $\tilde{p}(\mathcal{D})$ also collapses to uniform, which aligns well intuitively. An example of label distribution for 10 clients and their $p(\mathcal{D})$ s and $\tilde{p}(\mathcal{D})$ s are provided in Figure 3.

We measure the global and local accuracy varies on $p(\mathcal{D})$ and $\tilde{p}(\mathcal{D})$, as in Figure 4. After local training, the local models are well-fitted towards $p(\mathcal{D})$ (Figure 4a), and the aggregated global model also performs well on it. On the other hand, the accuracy on $\tilde{p}(\mathcal{D})$ significantly drops, and the global model accuracy on it also degrades (Figure 4b).

To summarize, the knowledge on the out-local distribution $\tilde{p}(\mathcal{D})$ is prone to be forgotten in local training, resulting in the global model’s forgetting. Based on our findings, we hypothesize that forgetting could be the stumbling block in federated learning.

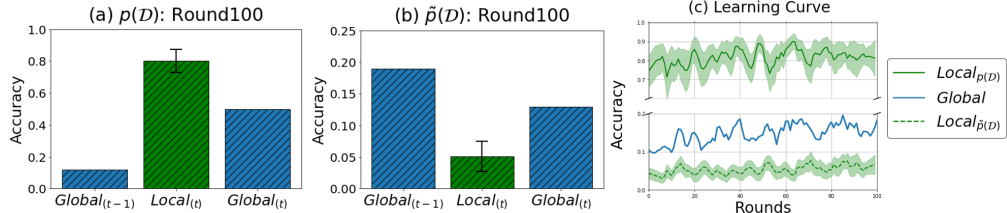


Figure 4: Accuracy of global model and sampled local models for $p(\mathcal{D})$ and $\tilde{p}(\mathcal{D})$ on CIFAR-10 ($\alpha=0.1$). The error bar stands for the standard deviation of the 10 sampled local clients. In (a) and (b), the global model accuracy for $p(\mathcal{D})$ and $\tilde{p}(\mathcal{D})$ is measured on their joint distributions from 10 sampled clients.

2.3 Forgetting and Local Drift

First empirically observed by [56], the deviation of local updates from the desirable global direction has been widely discussed as a major cause of slow and unstable convergence in heterogeneous federated learning [22, 32, 33]. Unfortunately, given that it is very difficult to analyze such drift, a common approach is to assume bounded dissimilarity between the local function gradients [21, 33].

One intriguing property of knowledge preservation on out-local distribution is that it corrects the local gradients towards the global direction. We define the gradient diversity Λ to measure the dissimilarity of local gradients and state the effect of knowledge preservation as follows:

Definition 2. For the uniformly weighted K clients, the gradient diversity Λ of local functions f^k towards the global function $f = \frac{1}{K} \sum_{k=1}^K f^k$ is defined as:

$$\Lambda := \frac{\frac{1}{K} \sum_{k=1}^K \|\nabla f^k\|^2}{\|\nabla f\|^2} \quad (8)$$

Here, $\Lambda \geq 1$ measures the alignment of gradient direction of the local function f^k 's w.r.t. the global function f . Note that the Λ becomes smaller as the directions of local function gradients ∇f^k 's become similar, e.g., if the magnitudes of the $\|\nabla f^k\|^2$'s are fixed, the smallest Λ is obtained when the direction of ∇f^k 's are identical.

Proposition 1. Suppose uniformly weighted K clients with in-local distribution $p^k = [p_1^k, \dots, p_C^k]$. If we assume the class-wise gradients g_c are orthogonal with uniform magnitude, increasing $\beta \leq C/2 - 1$ reduces the gradient diversity Λ from the local gradient $\nabla f^k = (p^k + \beta \tilde{p}^k) \cdot g$ with the ratio:

$$\frac{\partial \Lambda}{\partial \beta} \leq -\frac{M_{K,C,p}}{(1+\beta)^2}. \quad (9)$$

where β stands for the effect of knowledge preservation on the out-local distribution \tilde{p}^k . The $M_{K,C,p} > 0$ is a constant term consists of K , C , and $(p^k)_{k=1}^K$,

The proof is given in [Appendix N](#). Note that here we treat f^k as a sum of class-wise losses $\sum_c p_c^k \mathcal{L}_c$, where $\mathcal{L}_c = \mathbb{E}_{x|y=c} [\mathcal{L}(x; w)]$ is the loss on the specific class c . When $\beta = 0$, there is no regularization to preserve out-distribution knowledge, so the local model only needs to fit on the in-local distribution p^k . The above proposition suggests that the preserved knowledge on out-local distribution \tilde{p}^k (i.e., as β increases) guides the local gradient directions to be more aligned towards the global gradient, reducing the gradient diversity Λ . Such forgetting perspective provides the opportunity to handle the data heterogeneity at the model's prediction level.

3 FedNTD: Federated Not-True Distillation

In this section, we propose Federated Not-True Distillation (FedNTD) and its key features. The core idea of FedNTD is to preserve the global view only for the not-true classes. More specifically, FedNTD conducts local-side distillation by the linearly combined loss function \mathcal{L} between the cross-entropy loss \mathcal{L}_{CE} and the not-true distillation loss \mathcal{L}_{NTD} :

$$\mathcal{L} = \mathcal{L}_{CE}(q^l, \mathbf{1}_y) + \beta \cdot \mathcal{L}_{NTD}(\tilde{q}_\tau^l, \tilde{q}_\tau^g). \quad (10)$$

Here, the hyperparameter β stands for the strength of knowledge preservation on the out-local distribution. Then, the not-true distillation loss \mathcal{L}_{NTD} is defined as the KL-Divergence loss between the not-true softmax prediction vector \tilde{q}_τ^l and \tilde{q}_τ^g as follows:

$$\mathcal{L}_{NTD}(\tilde{q}_\tau^l, \tilde{q}_\tau^g) = - \sum_{c=1, c \neq y}^C \tilde{q}_\tau^g(c) \log \left[\frac{\tilde{q}_\tau^l(c)}{\tilde{q}_\tau^g(c)} \right], \text{ where } \begin{cases} \tilde{q}_\tau^l(c) = \frac{\exp(z_c^l/\tau)}{\sum_{\tilde{c} \neq y}^C \exp(z_{\tilde{c}}^l/\tau)} & (\forall c \neq y). \\ \tilde{q}_\tau^g(c) = \frac{\exp(z_c^g/\tau)}{\sum_{\tilde{c} \neq y}^C \exp(z_{\tilde{c}}^g/\tau)} \end{cases} \quad (11)$$

which take softmax with temperature τ only for the not-true class logits. [Figure 5](#) illustrates how the not-true distillation works given a sample x . Note that ignoring the true-class logits makes gradient signal of \mathcal{L}_{NTD} to the true-class as 0. The detailed algorithm is provided in [Appendix B](#).

We now explain how learning to minimize \mathcal{L}_{NTD} preserves global knowledge on out-local distribution $\tilde{p}(\mathcal{D})$. Since it is well-known that KL-Divergence loss on the softmax outputs acts as matching their logits vectors to close their distance [23, 44, 47], We start from a Mean-Squared Error (MSE) loss on the logits to simplify the discussion. Although not rigorous, this gives enough intuition to understand the effect of not-true distillation. An experimental validation is provided in [Appendix J](#).

Suppose there are N number of data points in the local dataset \mathcal{D} . The accumulated MSE loss \mathcal{L}_{MSE} between z_i^c , the class c logits of data x_i , and its reference logits $z_{i,\text{ref}}^c$ to be matched for is:

$$\mathcal{L}_{\text{MSE}} = \frac{1}{N\mathcal{C}} \sum_{i=1}^N \sum_{c=1}^{\mathcal{C}} (z_i^c - z_{i,\text{ref}}^c)^2. \quad (12)$$

By splitting the square term for the *true* and *not-true* classes, the term becomes:

$$\mathcal{L}_{\text{MSE}}^{\text{true}} = \frac{1}{N} \sum_{i=1}^N \sum_{c=y_i}^{\mathcal{C}} (z_i^c - z_{i,\text{ref}}^c)^2, \quad \mathcal{L}_{\text{MSE}}^{\text{not-true}} = \frac{1}{N(\mathcal{C}-1)} \sum_{i=1}^N \sum_{c' \neq y_i}^{\mathcal{C}} (z_i^{c'} - z_{i,\text{ref}}^{c'})^2. \quad (13)$$

Proposition 2. Consider the in-local distribution $p(\mathcal{D}) = [p_1 \dots p_{\mathcal{C}}]$ such that $p_c = \frac{|\mathcal{S}_c|}{N}$ and its out-local distribution $\tilde{p}(\mathcal{D}) = [\tilde{p}_1, \dots, \tilde{p}_{\mathcal{C}}]$, where \mathcal{S}_c is the set of indices satisfying $y_i = c$. Then the $\mathcal{L}_{\text{MSE}}^{\text{true}}$ and $\mathcal{L}_{\text{MSE}}^{\text{not-true}}$ each are equivalent to the weighted sum on $p(\mathcal{D})$ and $\tilde{p}(\mathcal{D})$ as

$$\mathcal{L}_{\text{MSE}}^{\text{true}} = \sum_{c=1}^{\mathcal{C}} p_c \left[\frac{\sum_{i \in \mathcal{S}_c} (z_i^c - z_{i,\text{ref}}^c)^2}{|\mathcal{S}_c|} \right], \quad \mathcal{L}_{\text{MSE}}^{\text{not-true}} = \sum_{c=1}^{\mathcal{C}} \tilde{p}_c \left[\frac{\sum_{i \notin \mathcal{S}_c} (z_i^c - z_{i,\text{ref}}^c)^2}{\sum_{c' \neq c} |\mathcal{S}_{c'}|} \right]. \quad (14)$$

where the term in $[\cdot]$ represents the normalized logits MSE for each class.

With a minor amount of calculation from [Equation 13](#), we derive the above proposition. The derivation is provided in [Appendix O](#). The proposition suggests that matching the true-class and the not-true class logits collapses to the loss on the in-local distribution $p(\mathcal{D})$ and the out-local distribution $\tilde{p}(\mathcal{D})$.

In the loss function of our FedNTD ([Equation 10](#)), we attain the new knowledge on the in-local distribution by following the true-class signals from the labeled data in local datasets using the \mathcal{L}_{CE} . In the meanwhile, we preserve the previous knowledge on the out-local distribution by following the global model's perspective, corresponding to the not-true class signals, using the \mathcal{L}_{NTD} . Here, the hyperparameter β controls the trade-off between learning on the new knowledge and preserving previous knowledge. This resembles to *stability-plasticity dilemma* [\[40\]](#) in continual learning, where the learning methods must balance retaining knowledge from previous tasks while learning new knowledge for the current task [\[37\]](#).

4 Experiment

4.1 Experimental Setup

We test our algorithm on MNIST [\[11\]](#), CIFAR-10 [\[27\]](#), CIFAR-100 [\[27\]](#), and CINIC-10 [\[10\]](#). We distribute the data to 100 clients and randomly sample clients with a ratio of 0.1. For CINIC-10, we use 200 clients with a sampling ratio of 0.05. We use a momentum SGD with an initial learning rate of 0.1, and the momentum is set as 0.9. The learning rate is decayed with a factor of 0.99 at each round, and a weight decay of 1e-5 is applied. We adopt two different NIID partition strategies:

- (i) **Sharding** [\[39\]](#): sort the data by label and divide the data into same-sized shards, and control the heterogeneity by s , the number of shards per user. In this strategy only considers the statistical heterogeneity as the dataset size is identical for each client. We set s as MNIST ($s = 2$), CIFAR-10 ($s \in \{2, 3, 5, 10\}$), CIFAR-100 ($s = 10$), and CINIC-10 ($s = 2$)).
- (ii) **Latent Dirichlet Allocation (LDA)** [\[36, 49\]](#): assigns partition of class c by sampling $p_c \sim \text{Dir}(\alpha)$. In this strategy, both the distribution and dataset size are different for each client. We set α as MNIST ($\alpha = 0.1$), CIFAR-10 ($\alpha \in \{0.05, 0.1, 0.3, 0.5\}$), CIFAR-100 ($\alpha = 0.1$), and CINIC-10 ($\alpha = 0.1$)

More details on model, datasets, hyperparameters, and partition strategies are provided in [Appendix C](#).

4.2 Performance on Data Heterogeneity

We compare our FedNTD with various existing works. The results are provided in [Table 1](#). As reported in [\[29\]](#), even the state-of-the-art methods perform well only in specific setups, and their performance often deteriorates below FedAvg. However, our FedNTD consistently outperforms the baselines on all setups, achieving state-of-the-art results in most cases.

For each experiment in [Table 1](#), we also report the forgetting \mathcal{F} in the parenthesis along with the accuracy. Note that the smaller \mathcal{F} value indicates the global model less forgets the previous knowledge. We find that the performance in federated learning is closely related to forgetting, with the performance improving as the forgetting reduces. *We believe that the gain from the prior works is actually from the forgetting prevention in their own ways.*

Table 1: Accuracy@1 (%) on MNIST [11], CIFAR-10 [27], CIFAR-100 [27], and CINIC-10 [10]. The values in the parenthesis are forgetting measure \mathcal{F} . The arrow (\downarrow , \uparrow) shows the comparison to the FedAvg. The standard deviation of each experiment is provided in Appendix E.

Method	NIID Partition Strategy : Sharding					
	MNIST		CIFAR-10		CIFAR-100 CINIC-10	
	$s = 2$	$s = 3$	$s = 5$	$s = 10$		
FedAvg [39]	78.63 _(0.20)	40.14 _(0.59)	51.10 _(0.46)	57.17 _(0.37)	64.91 _(0.26)	25.57 _(0.49) 39.64 _(0.59)
FedCurv [45]	78.56 _(0.21) \downarrow	44.52 _(0.53) \uparrow	49.00 _(0.47) \downarrow	54.61 _(0.39) \downarrow	62.19 _(0.27) \downarrow	22.89 _(0.49) \downarrow 40.45 _(0.57) \uparrow
FedAvgM [19]	80.81 _(0.18) \uparrow	37.30 _(0.61) \downarrow	50.80 _(0.46) \downarrow	63.53 _(0.32) \uparrow	69.36 _(0.24) \uparrow	28.22 _(0.46) \uparrow 36.04 _(0.62) \downarrow
FedProx [32]	78.26 _(0.21) \downarrow	41.48 _(0.57) \uparrow	51.65 _(0.45) \uparrow	56.88 _(0.37) \downarrow	64.65 _(0.25) \downarrow	25.10 _(0.49) \downarrow 41.47 _(0.57) \uparrow
FedNova [50]	77.04 _(0.21) \downarrow	42.62 _(0.56) \uparrow	52.03 _(0.44) \uparrow	62.14 _(0.30) \uparrow	66.97 _(0.20) \uparrow	26.96 _(0.41) \uparrow 42.55 _(0.56) \uparrow
SCAFFOLD [21]	81.05 _(0.17) \uparrow	44.60 _(0.53) \uparrow	54.26 _(0.39) \uparrow	65.74 _(0.23) \uparrow	68.97 _(0.16) \uparrow	30.82 _(0.36) \uparrow 42.66 _(0.54) \uparrow
MOON [30]	76.56 _(0.23) \downarrow	38.51 _(0.60) \downarrow	50.47 _(0.47) \downarrow	56.69 _(0.39) \downarrow	65.30 _(0.25) \uparrow	25.29 _(0.48) \downarrow 37.07 _(0.62) \downarrow
FedNTD (Ours)	84.44 _(0.13) \uparrow	52.61 _(0.43) \uparrow	58.18 _(0.34) \uparrow	64.93 _(0.23) \uparrow	68.56 _(0.15) \uparrow	31.69 _(0.32) \uparrow 48.07 _(0.48) \uparrow

Method	NIID Partition Strategy : LDA					
	MNIST		CIFAR-10		CIFAR-100 CINIC-10	
	$\alpha = 0.05$	$\alpha = 0.1$	$\alpha = 0.3$	$\alpha = 0.5$		
FedAvg [39]	79.73 _(0.19)	28.24 _(0.71)	46.49 _(0.51)	57.24 _(0.36)	62.53 _(0.28)	30.69 _(0.32) 38.14 _(0.60)
FedCurv [45]	78.72 _(0.20) \downarrow	33.64 _(0.66) \uparrow	44.26 _(0.53) \downarrow	54.93 _(0.38) \downarrow	59.37 _(0.30) \downarrow	29.16 _(0.32) \downarrow 36.69 _(0.61) \downarrow
FedAvgM [19]	81.05 _(0.18) \uparrow	13.70 _(0.86) \downarrow	42.39 _(0.55) \downarrow	62.89 _(0.32) \uparrow	66.96 _(0.26) \uparrow	34.43 _(0.32) \uparrow 30.79 _(0.68) \downarrow
FedProx [32]	79.25 _(0.19) \downarrow	37.19 _(0.62) \uparrow	47.65 _(0.49) \uparrow	57.35 _(0.35) \uparrow	62.39 _(0.27) \downarrow	30.60 _(0.32) \downarrow 39.47 _(0.58) \uparrow
FedNova [50]	60.37 _(0.38) \downarrow	10.00 (<i>Failed</i>) \downarrow	28.06 _(0.71) \downarrow	57.44 _(0.35) \uparrow	64.65 _(0.23) \uparrow	32.15 _(0.28) \uparrow 30.44 _(0.68) \downarrow
SCAFFOLD [21]	71.57 _(0.26) \downarrow	10.00 (<i>Failed</i>) \downarrow	23.12 _(0.74) \downarrow	62.01 _(0.29) \uparrow	66.16 _(0.19) \uparrow	33.68 _(0.25) \uparrow 28.78 _(0.69) \downarrow
MOON [30]	78.95 _(0.20) \downarrow	28.35 _(0.71) \uparrow	44.77 _(0.53) \downarrow	58.38 _(0.35) \uparrow	63.10 _(0.27) \uparrow	30.64 _(0.32) \downarrow 37.92 _(0.61) \downarrow
FedNTD (Ours)	81.34 _(0.17) \uparrow	40.17 _(0.58) \uparrow	54.42 _(0.42) \uparrow	62.42 _(0.29) \uparrow	66.12 _(0.19) \uparrow	32.37 _(0.26) \uparrow 46.24 _(0.50) \uparrow

We emphasize that the prior works to learn from heterogeneous locals often require *statefulness* (i.e., clients should be repeatedly sampled with identification) [30, 50], *additional communication cost* [21], or *auxiliary data* [35]. However, our FedNTD neither compromise any potential privacy issue nor requires additional communication burden. A brief comparison is provided in Appendix F.

We further conduct experiments on the effect of local epochs and client sampling ratio is in Appendix G, the advantage of not-true distillation over knowledge distillation in Appendix H, and the effect of hyperparameters of FedNTD in Appendix I. In the next section, we analyze how the knowledge preservation of FedNTD benefits on the federated learning.

5 Knowledge preservation of FedNTD

In Figure 7, we present the test accuracy on diverse heterogeneity levels. Although both FedAvg and FedNTD show little change in local accuracy on in-local distribution $p(x)$, FedNTD significantly improves the local accuracy on out-local distribution $\tilde{p}(x)$, which implies it prevents forgetting. Along with it, the test accuracy of the global model also substantially improves. These gaps are enlarged when the number of local epochs becomes greater, where the local models much deviate from the global model. The accuracy curves during local training are in Figure 6. It shows that fitting on the local distribution rapidly leads to forgetting on out-local distribution, But FedNTD effectively relieves this tendency without hurting the learning ability towards the in-local distribution.

Our interest is how the FedNTD’s knowledge preservation on out-local distribution benefits on the federated learning, despite of little change of its performance on in-local distribution. To figure it out, we analyze the local models in FedNTD after local training, and suggest two main reasons for it as:

- **Weight Alignment:** How much the semantics of each weight is preserved?
- **Weight Divergence:** How far the local weights drift from the global model?

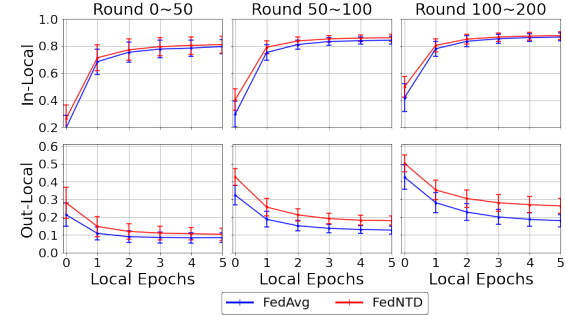


Figure 6: Accuracy on CIFAR-10 ($s=2$) in *Local Training*. The error bar stands for the standard deviation on clients.

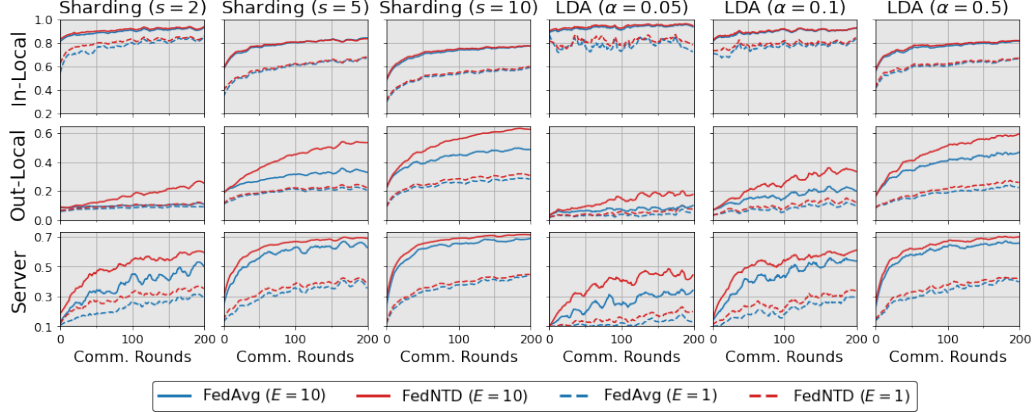


Figure 7: Learning curves of FedAvg [39] (blue line) and our FedNTD (red line) on CIFAR-10 with various heterogeneity setups for local epochs $E \in \{1, 10\}$. (1st and 2nd row) : Local test accuracy on in-local distribution $p(x)$ and out-local distribution $\tilde{p}(x)$. (3rd row): Global server test accuracy.

5.1 Weight Alignment

In recent studies, it has been suggested that there is a mismatch of semantic information encoded in the weight parameters across local models, even for the same coordinates (i.e., same position) [49, 54, 55]. As the current aggregation scheme averages weights of the identical coordinates, matching the semantic alignment across local models plays an important role in global convergence.

To analyze the semantic alignment of each parameter, we identify the individual neuron’s class preference by which class has the largest activation output on average. We then measure the alignment for a layer between two different models as the proportion of neurons that the class preference is matched for each other. The result is provided in Table 2.

While FedAvg and FedNTD show little difference in the IID case, FedNTD significantly enhances the alignment in the NIID cases. The visualized results are in Appendix K, with more details on how the alignment is measured. We further analyze the change of feature after local training using a unit hypersphere in Appendix L and T-SNE in Appendix M.

Table 2: Alignment of last two fc-layers for Distributed Global (DG), 10 Locals (L), and Aggregated Global (AG) models on CIFAR-10 datasets for IID and NIID (Sharding $s = 2$, LDA $\alpha = 0.05$) at round 200.

Layer	Alignment	IID		NIID ($s = 2$)		NIID ($\alpha = 0.05$)	
		FedAvg	FedNTD	FedAvg	FedNTD	FedAvg	FedNTD
Linear_1 (dim: 512)	$W_G^{(t-1)}$ vs. $W_L^{(t)}$	0.679	0.668	0.635	0.703	0.597	0.756
	$W_G^{(t-1)}$ vs. $W_G^{(t)}$	0.850	0.830	0.787	0.871	0.670	0.856
Linear_1 (dim: 128)	$W_G^{(t-1)}$ vs. $W_L^{(t)}$	0.771	0.765	0.488	0.552	0.512	0.730
	$W_G^{(t-1)}$ vs. $W_G^{(t)}$	0.898	0.906	0.609	0.836	0.586	0.859

5.2 Weight Divergence

The knowledge preservation by FedNTD leads the global model to predict each class more evenly. Here we describe how the global model with even prediction performance stabilizes the weight divergence. Consider a model fitted on a specific original distribution, and now it is trained on a new distribution. Then the weight distance between the original model and fitted model increases as the distance between the original distribution and new distribution grows.

We argue that if the distance between the global model’s underlying distribution and local distributions is close, the moved distance between the global model and local models also becomes close. If we assume the local distributions are generated arbitrarily, the most robust choice for the global model’s underlying distribution is a uniform distribution. We formally rephrase our argument as the follows:

Proposition 3. Let $\mathbb{P} : \Delta_C \rightarrow \mathbb{R}_{\geq 0}$ be the probability measure for the client’s local distribution and Π be the set of measure in the hypothesis. Assume that the class-wise loss $\mathcal{L}_c(w) = \mathbb{E}_{x|y=c}[\mathcal{L}(x; w)]$ is λ -smooth and w_c be a optimum of \mathcal{L}_c . Then the loss \mathcal{L} of the client with distribution p becomes:

$$\mathcal{L}(w) = \sum_c p_c \mathcal{L}_c(w) \leq \sum_c p_c \mathcal{L}_c(w_c) + \frac{1}{2} \lambda \sum_c p_c \|w - w_c\|^2. \quad (15)$$

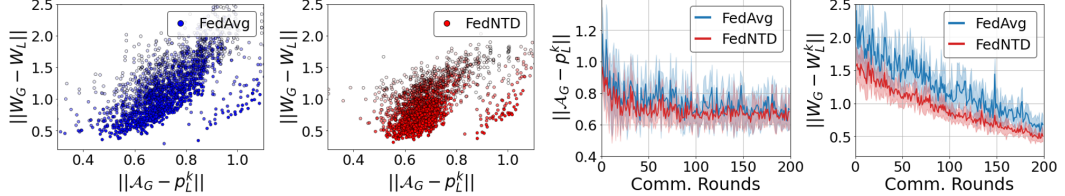


Figure 8: Distances for weights and distributions on CIFAR10 ($s=2$). (a), (b): The relationship between two distances. The opacity is higher for later rounds. (c), (d): The measured distances for 200 rounds.

Then for arbitrary $\mathbb{P} \in \Pi$, the uniform distribution attains the minimax value:

$$\text{unif.dist} \in \operatorname{argmin}_{p \in \Delta_C} \sup_{\mathbb{P} \in \Pi} \mathbb{E}_{p' \sim \mathbb{P}} [\|w_{p'} - w_p\|], \text{ where } w_p = \sum_c p_c w_c. \quad (16)$$

The proof is provided in Appendix Q. Although the global model’s underlying distribution is unknown, the normalized class-wise accuracy vector is a handy approximation for it as: $\mathcal{A}_G = \frac{1}{A} \cdot [a_1, \dots, a_C]$, where A is the global model’s test accuracy and a_c is its class-wise accuracy on the class c .

The results in Figure 8 empirically validate our argument. There is a strong correlation between weight divergence $\|w - w_k\|$ (for global model w and client k ’s local model w_k) and distribution distance $\|\mathcal{A}_G - p_k\|$ (for client k ’s distribution p_k). By providing a better starting point for local training, FedNTD effectively stabilizes the weight divergence.

6 Related Work

Federated Learning is proposed to update a global model while the local data is kept in clients’ devices [25, 26]. The de facto standard algorithm is FedAvg [39], which aggregates trained local models by averaging their parameters. Although its effectiveness has been largely discussed in i.i.d. settings [46, 51], many algorithms obtain the sub-optimal when the distributed data is heterogeneous [33, 56]. Until recently, a wide range of variants of FedAvg has been proposed to overcome such a problem. One line of work is the *local-side* modification. For example, Fedprox [32] adds a proximal term in local objective, and SCAFFOLD [21] uses control variates to correct the client-drift. Likewise, the *server-side* modification by post-training after aggregation is also considered in various works. For instance, FedDF [35] distills from an ensemble of local models via auxiliary data. FedMA [49] seek the optimal transport to match the layer-wise order of individual neurons. Our work is a local-side modification, which focuses on the local objective.

Continual Learning is a learning paradigm that updates a sequence of tasks [43, 48]. In continual learning, the main challenge is to avoid catastrophic forgetting [14], whereby training on the new task interferes with the previous tasks. Existing methods try to mitigate this problem by various strategies. In *Parameter-based* approaches, the importance of parameters for the previous task is measured to restrict their changes [3, 5, 24]. *Regularization-based* approaches [4, 34] introduce regularization terms to prevent forgetting. *Memory-based* approaches [6, 8] keep a small episodic memory from the previous tasks and replay it to maintain knowledge.

Knowledge Distillation is proposed to transfer knowledge from a model to another [15, 44]. In federated learning, a typical approach is using knowledge distillation to make the global model learn from the ensemble of local models [9, 28, 35, 57]. The local-side distillation is recently proposed in [58], which introduces a generator model and broadcasts to the clients at each round. However, the generator model requires extra communication burden, and the server should identify the local distribution to train the generator model. Instead, we focus on the forgetting issue and suggest that a simple variant of knowledge distillation surprisingly performs well on heterogeneity scenarios, without any additional resource requirements.

7 Conclusion

This study begins from an analogy to continual learning and suggests that forgetting could be a major concern in federated learning. In our observations, the knowledge outside of local distribution is prone to be forgotten in local training and is closely related to the unstable global convergence. To overcome this issue, we propose a simple yet effective algorithm, FedNTD, which conducts local-side distillation only for the not-true classes to prevent forgetting. FedNTD does not have any additional requirements, unlike previous approaches. We analyze the effect of FedNTD from various perspectives and demonstrate its benefits in federated learning.

References

- [1] Durmus Alp Emre Acar, Yue Zhao, Ramon Matas Navarro, Matthew Mattina, Paul N Whatmough, and Venkatesh Saligrama. Federated learning based on dynamic regularization. *arXiv preprint arXiv:2111.04263*, 2021.
- [2] Mohammed Aledhari, Rehma Razzak, Reza M Parizi, and Fahad Saeed. Federated learning: A survey on enabling technologies, protocols, and applications. *IEEE Access*, 8:140699–140725, 2020.
- [3] Rahaf Aljundi, Francesca Babiloni, Mohamed Elhoseiny, Marcus Rohrbach, and Tinne Tuytelaars. Memory aware synapses: Learning what (not) to forget. In *Proceedings of the European Conference on Computer Vision (ECCV)*, pages 139–154, 2018.
- [4] Sungmin Cha, Hsiang Hsu, Taebaek Hwang, Flavio P Calmon, and Taesup Moon. Cpr: Classifier-projection regularization for continual learning. *arXiv preprint arXiv:2006.07326*, 2020.
- [5] Arslan Chaudhry, Puneet K Dokania, Thalaiyasingam Ajanthan, and Philip HS Torr. Riemannian walk for incremental learning: Understanding forgetting and intransigence. In *Proceedings of the European Conference on Computer Vision (ECCV)*, pages 532–547, 2018.
- [6] Arslan Chaudhry, Albert Gordo, Puneet Kumar Dokania, Philip Torr, and David Lopez-Paz. Using hindsight to anchor past knowledge in continual learning. *arXiv preprint arXiv:2002.08165*, 2(7), 2020.
- [7] Arslan Chaudhry, Naeemullah Khan, Puneet K Dokania, and Philip HS Torr. Continual learning in low-rank orthogonal subspaces. *arXiv preprint arXiv:2010.11635*, 2020.
- [8] Arslan Chaudhry, Marc’Aurelio Ranzato, Marcus Rohrbach, and Mohamed Elhoseiny. Efficient lifelong learning with a-gem. *arXiv preprint arXiv:1812.00420*, 2018.
- [9] Hong-You Chen and Wei-Lun Chao. Fedbe: Making bayesian model ensemble applicable to federated learning. *arXiv preprint arXiv:2009.01974*, 2020.
- [10] Luke N Darlow, Elliot J Crowley, Antreas Antoniou, and Amos J Storkey. Cinic-10 is not imagenet or cifar-10. *arXiv preprint arXiv:1810.03505*, 2018.
- [11] Li Deng. The mnist database of handwritten digit images for machine learning research. *IEEE Signal Processing Magazine*, 29(6):141–142, 2012.
- [12] Terrance DeVries and Graham W Taylor. Improved regularization of convolutional neural networks with cutout. *arXiv preprint arXiv:1708.04552*, 2017.
- [13] Mehrdad Farajtabar, Navid Azizan, Alex Mott, and Ang Li. Orthogonal gradient descent for continual learning. In *International Conference on Artificial Intelligence and Statistics*, pages 3762–3773. PMLR, 2020.
- [14] Ian J Goodfellow, Mehdi Mirza, Da Xiao, Aaron Courville, and Yoshua Bengio. An empirical investigation of catastrophic forgetting in gradient-based neural networks. *arXiv preprint arXiv:1312.6211*, 2013.
- [15] Jianping Gou, Baosheng Yu, Stephen J Maybank, and Dacheng Tao. Knowledge distillation: A survey. *International Journal of Computer Vision*, 129(6):1789–1819, 2021.
- [16] Chaoyang He, Songze Li, Jinhyun So, Xiao Zeng, Mi Zhang, Hongyi Wang, Xiaoyang Wang, Praneeth Vepakomma, Abhishek Singh, Hang Qiu, et al. Fedml: A research library and benchmark for federated machine learning. *arXiv preprint arXiv:2007.13518*, 2020.
- [17] Geoffrey Hinton, Oriol Vinyals, and Jeff Dean. Distilling the knowledge in a neural network. *arXiv preprint arXiv:1503.02531*, 2015.
- [18] Tzu-Ming Harry Hsu, Hang Qi, and Matthew Brown. Measuring the effects of non-identical data distribution for federated visual classification. *arXiv preprint arXiv:1909.06335*, 2019.
- [19] Tzu-Ming Harry Hsu, Hang Qi, and Matthew Brown. Measuring the effects of non-identical data distribution for federated visual classification. *arXiv preprint arXiv:1909.06335*, 2019.
- [20] Peter Kairouz, H Brendan McMahan, Brendan Avent, Aurélien Bellet, Mehdi Bennis, Arjun Nitin Bhagoji, Keith Bonawitz, Zachary Charles, Graham Cormode, Rachel Cummings, et al. Advances and open problems in federated learning. *arXiv preprint arXiv:1912.04977*, 2019.

- [21] Sai Praneeth Karimireddy, Satyen Kale, Mehryar Mohri, Sashank Reddi, Sebastian Stich, and Ananda Theertha Suresh. Scaffold: Stochastic controlled averaging for federated learning. In *International Conference on Machine Learning*, pages 5132–5143. PMLR, 2020.
- [22] Ahmed Khaled, Konstantin Mishchenko, and Peter Richtárik. Tighter theory for local sgd on identical and heterogeneous data. In *International Conference on Artificial Intelligence and Statistics*, pages 4519–4529. PMLR, 2020.
- [23] Taehyeon Kim, Jaehoon Oh, NakYil Kim, Sangwook Cho, and Se-Young Yun. Comparing kullback-leibler divergence and mean squared error loss in knowledge distillation. *arXiv preprint arXiv:2105.08919*, 2021.
- [24] James Kirkpatrick, Razvan Pascanu, Neil Rabinowitz, Joel Veness, Guillaume Desjardins, Andrei A Rusu, Kieran Milan, John Quan, Tiago Ramalho, Agnieszka Grabska-Barwinska, et al. Overcoming catastrophic forgetting in neural networks. *Proceedings of the national academy of sciences*, 114(13):3521–3526, 2017.
- [25] Jakub Konečný, H Brendan McMahan, Daniel Ramage, and Peter Richtárik. Federated optimization: Distributed machine learning for on-device intelligence. *arXiv preprint arXiv:1610.02527*, 2016.
- [26] Jakub Konečný, H Brendan McMahan, Felix X Yu, Peter Richtárik, Ananda Theertha Suresh, and Dave Bacon. Federated learning: Strategies for improving communication efficiency. *arXiv preprint arXiv:1610.05492*, 2016.
- [27] Alex Krizhevsky, Vinod Nair, and Geoffrey Hinton. Cifar-10 and cifar-100 datasets. URL: <https://www.cs.toronto.edu/kriz/cifar.html>, 6, 2009.
- [28] Daliang Li and Junpu Wang. Fedmd: Heterogenous federated learning via model distillation. *arXiv preprint arXiv:1910.03581*, 2019.
- [29] Qinbin Li, Yiqun Diao, Quan Chen, and Bingsheng He. Federated learning on non-iid data silos: An experimental study. *arXiv preprint arXiv:2102.02079*, 2021.
- [30] Qinbin Li, Bingsheng He, and Dawn Song. Model-contrastive federated learning. In *Proceedings of the IEEE/CVF Conference on Computer Vision and Pattern Recognition*, pages 10713–10722, 2021.
- [31] Tian Li, Anit Kumar Sahu, Ameet Talwalkar, and Virginia Smith. Federated learning: Challenges, methods, and future directions. *IEEE Signal Processing Magazine*, 37(3):50–60, 2020.
- [32] Tian Li, Anit Kumar Sahu, Manzil Zaheer, Maziar Sanjabi, Ameet Talwalkar, and Virginia Smith. Federated optimization in heterogeneous networks. *Proceedings of Machine Learning and Systems*, 2:429–450, 2020.
- [33] Xiang Li, Kaixuan Huang, Wenhao Yang, Shusen Wang, and Zhihua Zhang. On the convergence of fedavg on non-iid data. *arXiv preprint arXiv:1907.02189*, 2019.
- [34] Zhizhong Li and Derek Hoiem. Learning without forgetting. *IEEE transactions on pattern analysis and machine intelligence*, 40(12):2935–2947, 2017.
- [35] Tao Lin, Lingjing Kong, Sebastian U Stich, and Martin Jaggi. Ensemble distillation for robust model fusion in federated learning. *arXiv preprint arXiv:2006.07242*, 2020.
- [36] Mi Luo, Fei Chen, Dapeng Hu, Yifan Zhang, Jian Liang, and Jiashi Feng. No fear of heterogeneity: Classifier calibration for federated learning with non-iid data. *arXiv preprint arXiv:2106.05001*, 2021.
- [37] Marc Masana, Xiaolei Liu, Bartłomiej Twardowski, Mikel Menta, Andrew D Bagdanov, and Joost van de Weijer. Class-incremental learning: survey and performance evaluation on image classification. *arXiv preprint arXiv:2010.15277*, 2020.
- [38] Michael McCloskey and Neal J Cohen. Catastrophic interference in connectionist networks: The sequential learning problem. In *Psychology of learning and motivation*, volume 24, pages 109–165. Elsevier, 1989.
- [39] Brendan McMahan, Eider Moore, Daniel Ramage, Seth Hampson, and Blaise Aguera y Arcas. Communication-efficient learning of deep networks from decentralized data. In *Artificial Intelligence and Statistics*, pages 1273–1282. PMLR, 2017.

- [40] Martial Mermilliod, Aurélia Bugaiska, and Patrick Bonin. The stability-plasticity dilemma: Investigating the continuum from catastrophic forgetting to age-limited learning effects. *Frontiers in psychology*, 4:504, 2013.
- [41] German I Parisi, Ronald Kemker, Jose L Part, Christopher Kanan, and Stefan Wermter. Continual lifelong learning with neural networks: A review. *Neural Networks*, 113:54–71, 2019.
- [42] Adam Paszke, Sam Gross, Francisco Massa, Adam Lerer, James Bradbury, Gregory Chanan, Trevor Killeen, Zeming Lin, Natalia Gimelshein, Luca Antiga, Alban Desmaison, Andreas Kopf, Edward Yang, Zachary DeVito, Martin Raison, Alykhan Tejani, Sasank Chilamkurthy, Benoit Steiner, Lu Fang, Junjie Bai, and Soumith Chintala. Pytorch: An imperative style, high-performance deep learning library. In H. Wallach, H. Larochelle, A. Beygelzimer, F. d’Alché-Buc, E. Fox, and R. Garnett, editors, *Advances in Neural Information Processing Systems 32*, pages 8024–8035. Curran Associates, Inc., 2019.
- [43] Mark B Ring. Child: A first step towards continual learning. In *Learning to learn*, pages 261–292. Springer, 1998.
- [44] Fabian Ruffy and Karanbir Chahal. The state of knowledge distillation for classification. *arXiv preprint arXiv:1912.10850*, 2019.
- [45] Neta Shoham, Tomer Avidor, Aviv Keren, Nadav Israel, Daniel Benditkis, Liron Mor-Yosef, and Itai Zeitak. Overcoming forgetting in federated learning on non-iid data. *arXiv preprint arXiv:1910.07796*, 2019.
- [46] Sebastian U Stich. Local sgd converges fast and communicates little. *arXiv preprint arXiv:1805.09767*, 2018.
- [47] Jiaxi Tang, Rakesh Shivanna, Zhe Zhao, Dong Lin, Anima Singh, Ed H Chi, and Sagar Jain. Understanding and improving knowledge distillation. *arXiv preprint arXiv:2002.03532*, 2020.
- [48] Sebastian Thrun. Lifelong learning algorithms. In *Learning to learn*, pages 181–209. Springer, 1998.
- [49] Hongyi Wang, Mikhail Yurochkin, Yuekai Sun, Dimitris Papailiopoulos, and Yasaman Khazaeni. Federated learning with matched averaging. *arXiv preprint arXiv:2002.06440*, 2020.
- [50] Jianyu Wang, Qinghua Liu, Hao Liang, Gauri Joshi, and H Vincent Poor. Tackling the objective inconsistency problem in heterogeneous federated optimization. *arXiv preprint arXiv:2007.07481*, 2020.
- [51] Blake Woodworth, Kumar Kshitij Patel, Sebastian Stich, Zhen Dai, Brian Bullins, Brendan McMahan, Ohad Shamir, and Nathan Srebro. Is local sgd better than minibatch sgd? In *International Conference on Machine Learning*, pages 10334–10343. PMLR, 2020.
- [52] Qiang Yang, Yang Liu, Tianjian Chen, and Yongxin Tong. Federated machine learning: Concept and applications. *ACM Transactions on Intelligent Systems and Technology (TIST)*, 10(2):1–19, 2019.
- [53] Tehrim Yoon, Sumin Shin, Sung Ju Hwang, and Eunho Yang. Fedmix: Approximation of mixup under mean augmented federated learning. In *International Conference on Learning Representations*, 2021.
- [54] Fuxun Yu, Weishan Zhang, Zhuwei Qin, Zirui Xu, Di Wang, Chenchen Liu, Zhi Tian, and Xiang Chen. Fed2: Feature-aligned federated learning. In *Proceedings of the 27th ACM SIGKDD Conference on Knowledge Discovery & Data Mining*, pages 2066–2074, 2021.
- [55] Mikhail Yurochkin, Mayank Agarwal, Soumya Ghosh, Kristjan Greenewald, Nghia Hoang, and Yasaman Khazaeni. Bayesian nonparametric federated learning of neural networks. In *International Conference on Machine Learning*, pages 7252–7261. PMLR, 2019.
- [56] Yue Zhao, Meng Li, Liangzhen Lai, Naveen Suda, Damon Civin, and Vikas Chandra. Federated learning with non-iid data. *arXiv preprint arXiv:1806.00582*, 2018.
- [57] Yanlin Zhou, George Pu, Xiayao Ma, Xiaolin Li, and Dapeng Wu. Distilled one-shot federated learning. *arXiv preprint arXiv:2009.07999*, 2020.
- [58] Zhuangdi Zhu, Junyuan Hong, and Jiayu Zhou. Data-free knowledge distillation for heterogeneous federated learning. *arXiv preprint arXiv:2105.10056*, 2021.

A Table of Notations

Table 3: Table of Notations throughout the paper.

Indices:	
c, c'	index for classes ($c \in \{1, \dots, C\} = [\mathcal{C}]$)
i	index for data ($i \in \{1, \dots, N\} = [N]$)
k, k'	index for clients ($k \in \{1, \dots, K\} = [K]$ or $\in K^{(t)}$)
t	index for rounds ($t \in \{1, \dots, T\} = [T]$)
e	index for local epochs ($t \in \{1, \dots, E\} = [E]$)
Parameters:	
α	Parameter for the Dirichlet Distribution
s	The Number of shards per user
β	Hyperparameter for the distillation loss; generally controls the relative weight of divergence loss
τ	The temperature on the softmax
γ	Learning rate
Data and Weights:	
\mathcal{D}	whole dataset
\mathcal{D}^k	local dataset
x	datum
y	class label for datum
$w^{(t)}$	weight of the server model on the round t
$w_k^{(t)}$	weight of the k -th client model on the round t
$\ W_G - W_L\ $	Collection of L^1 -norm between server and client models, among all rounds.
Softmax Probabilities:	
q_τ^T / q_τ^S	The softened softmax probability of teacher/student model
q^g / q^l	The softmax probability on the server/client model
$\tilde{q}_\tau^g / \tilde{q}_\tau^l$	The softened softmax probability calculated without true-class logit on the server/client model
Class Distribution on Datasets:	
$p = [p_1, \dots, p_C]$	In-local distribution of dataset
$\tilde{p} = [\tilde{p}_1, \dots, \tilde{p}_C]$	Out-local distribution of dataset
Loss Functions:	
\mathcal{L}_{CE}	cross-entropy loss
\mathcal{L}_{KL}	Kullback-Leibler divergence
\mathcal{L}_{NTD}	Proposed Not-True Distillation Loss
Accuracy and Forgetting Measure:	
$\mathcal{A}_c^{(t)}$	Accuracy of the server model on the c -th class, at round t .
$\ \mathcal{A}_G - p_L^k\ $	Collection of L^1 -norm between <i>normalized</i> global accuracy and data distribution on each client, among all rounds.
\mathcal{F}	Backward Transfer (BwT). For the federated learning situation, we calculate this measure on the server model.

B Algorithm

Algorithm 1 Federated Not-True Distillation (FedNTD)

Input: total rounds T , local epochs E , dataset \mathcal{D} , sampled clients sets $K^{(t)} \subset K$ in round t , learning rate γ

Initialize $w^{(0)}$ for global server weight

for each communication round $t = 1, \dots, T$ **do**

- Server samples clients $K^{(t)}$ and broadcasts $\tilde{w}^{(t)} \leftarrow w^{(t)}$
- for** each client $k \in K^{(t)}$ **in parallel do**

 - for** Local Steps $e = 1 \dots E$ **do**

 - for** Batches $j = 1 \dots B$ **do**

 - $\tilde{w}_k^{(t)} \leftarrow \tilde{w}_k^{(t)} - \gamma \nabla_w \mathcal{L}(\tilde{w}_k^{(t)}; [\mathcal{D}^k]_j)$ Using [Equation 10]

 - end for**
 - end for**

 - end for**
 - Upload $\tilde{w}_k^{(t)}$ to server
 - Server Aggregation :** $w^{(t+1)} \leftarrow \frac{1}{|K^{(t)}|} \sum_{k \in K^{(t)}} \tilde{w}_k^{(t)}$

end for

Server output : w_T

C Experimental Setups

Here we provide details of our experimental setups. The code is implemented by PyTorch [42] and the overall code structure is based on FedML [16] library with some modifications.

C.1 Model Architecture

The model architecture used in our experiment is from [39], which is composed of two convolutional layers followed by max-pooling layers, and two fully connected layer. A similar architecture is used in [30, 36].

C.2 Datasets

We mainly used four benchmarks: MNIST [11], CIFAR-10 [27], CIFAR-100 [27], and CINIC-10 [10]. The details about each datasets and setups are described in Table 4. We augment the training data using Random Cropping, Horizontal Flipping, and Normalization. For MNIST, CIFAR-10, and CIFAR-100, we add Cutout [12] augmentation.

Table 4: Details datasets setups used in the experiment.

Datasets	MNIST	CIFAR-10	CIFAR-100	CINIC-10
Datasets Classes	10	10	100	10
Datasets Size	50,000	50,000	50,000	90,000
Number of Clients	100	100	100	200
Client Sampling Ratio	0.1	0.1	0.1	0.05
Local Epochs (E)	3	5	5	5
Batch Size (B)	50	50	50	50

C.3 Learning Setups

We use a momentum SGD optimizer with an initial learning rate of 0.1, and the momentum is set as 0.9. The momentum is only used in the local training, which implies the momentum information is not communicated to the server. The learning rate is decayed with a factor of 0.99 at each round, and a weight decay of 0.00001 is applied. In the motivational experiment in Section 3, we fix the learning rate as 0.01. Since we assume a synchronized federated learning scenario, parallel distributed learning is simulated by sequentially training the sampled clients and then aggregating them as a global model.

C.4 Algorithm Implementation Details

For the implemented algorithms, we search hyperparameters and choose the best among the candidates. The hyperparameters for each algorithm is in [Table 5](#).

[Table 5](#): Algorithm-specific hyperparameters used in the experiment.

Method	Hyperparameters	Searched Candidates
FedAvg [39]	None	None
FedCurv [45]	$s = 500, \lambda = 1.0$	$s \in \{250, 500\}, \lambda \in \{0.1, 0.5, 1.0\}$
FedAvgM [19]	$\beta = 0.7$	$\beta \in \{0.7, 0.9, 0.99\}$
FedProx [32]	$\mu = 0.1$	$\mu \in \{0.1, 0.5, 1.0\}$
FedNova [50]	None	None
SCAFFOLD [21]	None	None
MOON [30]	$\mu = 1.0, \tau = 0.5$	$\mu \in \{0.1, 0.5, 1.0\}, \tau \in \{0.1, 0.5, 1, 0\}$
FedNTD (Ours)		

C.5 Non-IID Partition Strategy

To widely address the heterogeneous federated learning scenarios, we distribute the data to the local clients with the following two strategies: (1) **Sharding** and (2) **Latent Dirichlet Allocation** (LDA).

Sharding In the Sharding strategy, we sort the data by label and divide it into the same-sized shards without overlapping. In detail, a shard contains $\frac{|D|}{N \times s}$ size of same class samples, where D is the total dataset size, N is the total number of clients, and s is the number of shards per user. Then, we distribute s number of shards to each client. s controls the heterogeneity of local data distribution. The heterogeneity level increases as the shard per user s becomes smaller and vice versa. Note that we only test the statistical heterogeneity (skewness of class distribution across the local clients) in the Sharding strategy, and the size of local datasets is identical.

Latent Dirichlet Allocation (LDA) IN LDA strategy, Each client k is allocated with $p_{c,k}$ proportion of the training samples of class c , where $p_c \sim \text{Dir}_K(\alpha)$ and α is the concentration parameter controlling the heterogeneity. The heterogeneity level increases as the concentration parameter α becomes smaller, and vice versa. Note that both the class distribution and local datasets sizes differ across the local clients in LDA strategy.

D Server Prediction Consistency

We extend the motivational experiment in Section 3.1 to the main experimental setups. Here, we plotted the *normalized* class-wise test accuracy for each case to identify the contribution of each class on the current accuracy. This helps observe the prediction consistency regardless of the highly fluctuating global server accuracy in the non-IID case. As in [Figure 9](#), FedNTD effectively preserves the knowledge from the previous rounds; thereby the global server model becomes to predict each class evenly much earlier than FedAvg. Note that we normalize the class-wise test accuracy as round-by-round manner, which makes the sum for each round as 1.0.

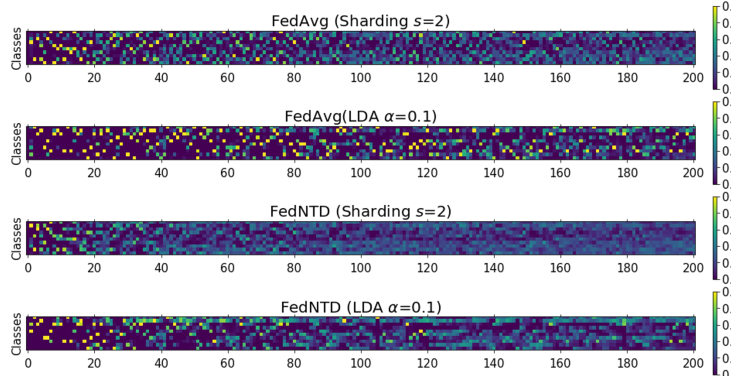


[Figure 9](#): Visualized server test accuracy of FedAvg and FedNTD on CIFAR-10 datasets.

E Experiment Table with Standard Deviation

Table 6: Accuracy@1 (%) on MNIST [11], CIFAR-10 [27], CIFAR-100 [27], and CINIC-10 [10]. The values in the parenthesis are the standard deviation. The arrow (\downarrow , \uparrow) shows the comparison to the FedAvg.

Method	IID Partition Strategy : Sharding					CIFAR-100	CINIC-10		
	MNIST		CIFAR-10						
	$s = 2$	$s = 3$	$s = 5$	$s = 10$					
FedAvg [39]	78.63 ± 0.42	40.14 ± 1.15	51.10 ± 0.11	57.17 ± 0.12	64.91 ± 0.69	25.57 ± 0.44	39.64 ± 0.78		
FedCurv [45]	$78.56 \pm 0.23 \downarrow$	$44.52 \pm 0.44 \uparrow$	$49.00 \pm 0.41 \downarrow$	$54.61 \pm 0.20 \downarrow$	$62.19 \pm 0.47 \downarrow$	$22.89 \pm 0.66 \downarrow$	$40.45 \pm 0.25 \uparrow$		
FedAvgM [19]	$80.81 \pm 0.20 \uparrow$	$37.30 \pm 0.21 \downarrow$	$50.80 \pm 2.05 \downarrow$	$63.53 \pm 1.46 \uparrow$	$69.36 \pm 0.18 \uparrow$	$28.22 \pm 0.01 \uparrow$	$36.04 \pm 1.29 \downarrow$		
FedProx [32]	$78.26 \pm 0.28 \downarrow$	$41.48 \pm 1.08 \uparrow$	$51.65 \pm 0.53 \uparrow$	$56.88 \pm 0.15 \downarrow$	$64.65 \pm 0.61 \downarrow$	$25.10 \pm 0.67 \downarrow$	$41.47 \pm 0.99 \uparrow$		
FedNova [50]	$77.04 \pm 0.98 \downarrow$	$42.62 \pm 1.32 \uparrow$	$52.03 \pm 1.49 \uparrow$	$62.14 \pm 0.74 \uparrow$	$66.97 \pm 0.39 \uparrow$	$26.96 \pm 0.59 \uparrow$	$42.55 \pm 0.10 \uparrow$		
SCAFFOLD [21]	$81.05 \pm 0.26 \uparrow$	$44.60 \pm 2.24 \uparrow$	$54.26 \pm 0.22 \uparrow$	$65.74 \pm 0.36 \uparrow$	$68.97 \pm 0.34 \uparrow$	$30.82 \pm 0.31 \uparrow$	$42.66 \pm 0.92 \uparrow$		
MOON [30]	$76.56 \pm 0.24 \downarrow$	$38.51 \pm 0.96 \downarrow$	$50.47 \pm 0.15 \downarrow$	$56.69 \pm 0.11 \downarrow$	$65.30 \pm 0.51 \downarrow$	$25.29 \pm 0.24 \downarrow$	$37.07 \pm 0.24 \downarrow$		
FedNTD (Ours)	$84.44 \pm 0.43 \uparrow$	$52.61 \pm 1.00 \uparrow$	$58.18 \pm 1.42 \uparrow$	$64.93 \pm 0.34 \uparrow$	$68.56 \pm 0.24 \uparrow$	$31.69 \pm 0.13 \uparrow$	$48.07 \pm 0.36 \uparrow$		

Method	IID Partition Strategy : LDA				CIFAR-100	CINIC-10		
	MNIST		CIFAR-10					
	$\alpha = 0.05$	$\alpha = 0.1$	$\alpha = 0.3$	$\alpha = 0.5$				
FedAvg [39]	79.73 ± 0.20	28.24 ± 3.11	46.49 ± 0.93	57.24 ± 0.21	62.53 ± 0.41	30.69 ± 0.27		
FedCurv [45]	$78.72 \pm 0.44 \downarrow$	$33.64 \pm 2.98 \uparrow$	$44.26 \pm 0.79 \downarrow$	$54.93 \pm 0.46 \downarrow$	$59.37 \pm 0.24 \downarrow$	$29.16 \pm 0.22 \downarrow$		
FedAvgM [19]	$81.05 \pm 0.54 \uparrow$	$13.70 \pm 0.00 \downarrow$	$42.39 \pm 0.87 \downarrow$	$62.89 \pm 0.64 \uparrow$	$66.96 \pm 0.43 \uparrow$	$34.43 \pm 0.39 \uparrow$		
FedProx [32]	$79.25 \pm 0.16 \downarrow$	$37.19 \pm 3.17 \uparrow$	$47.65 \pm 0.90 \uparrow$	$57.35 \pm 0.40 \uparrow$	$62.39 \pm 0.31 \downarrow$	$30.60 \pm 0.16 \downarrow$		
FedNova [50]	$60.37 \pm 2.71 \downarrow$	$10.00 \text{ (Failed)} \downarrow$	$28.06 \pm 0.12 \downarrow$	$57.44 \pm 1.68 \uparrow$	$64.65 \pm 0.34 \uparrow$	$32.15 \pm 0.13 \uparrow$		
SCAFFOLD [21]	$71.57 \pm 0.72 \downarrow$	$10.00 \text{ (Failed)} \downarrow$	$23.12 \pm 0.55 \downarrow$	$62.01 \pm 0.34 \uparrow$	$66.16 \pm 0.13 \uparrow$	$33.68 \pm 0.13 \uparrow$		
MOON [30]	$78.95 \pm 0.46 \downarrow$	$28.35 \pm 3.68 \uparrow$	$44.77 \pm 1.12 \downarrow$	$58.38 \pm 0.09 \uparrow$	$63.10 \pm 0.00 \uparrow$	$30.64 \pm 0.12 \downarrow$		
FedNTD (Ours)	$81.34 \pm 0.33 \uparrow$	$40.17 \pm 3.19 \uparrow$	$54.42 \pm 0.06 \uparrow$	$62.42 \pm 0.53 \uparrow$	$66.12 \pm 0.26 \uparrow$	$32.37 \pm 0.02 \uparrow$		

F Conceptual comparison to prior works

The conceptual illustration of federated distillation methods is in Figure 10. The existing algorithms either use additional local information (Figure 10a) or need an auxiliary (or proxy) data to conduct distillation. On the other hand, our proposed FedNTD does not have such constraints (Figure 10c).

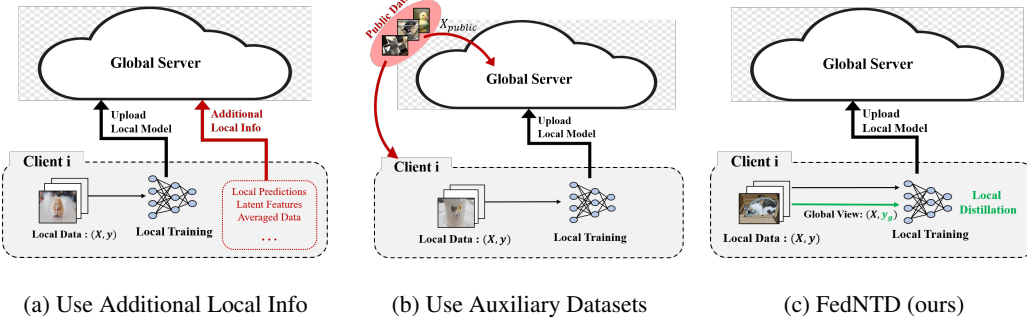


Figure 10: An overview of federated distillation methods.

Table 7: Additional resource requirements compared to FedAvg.

Method	No Additional Requirements on:		
	Statefulness?	Communication Cost?	Auxiliary Data?
FedEnsemble [35]	✓	✓	✗
FedBE [9]	✓	✗	✗
MOON [30]	✗	✓	✓
SCAFFOLD [21]	✗	✗	✓
FedNTD (Ours)	✓	✓	✓

G Additional Experiments

G.1 Effect of Local Epochs

Table 8: Accuracy@1 on CIFAR-10 (Sharding $s = 2$). The value in the parenthesis is the forgetting \mathcal{F} .

Method	IID Partition Strategy: Sharding ($s = 2$)				
	Local Epochs (E)				
	1	3	5	10	20
FedAvg [39]	29.49 (0.70)	34.49 (0.64)	40.14 (0.59)	50.08 (0.49)	56.93 (0.42)
FedProx [32]	29.44 (0.69) ↓	34.00 (0.64) ↓	41.48 (0.57) ↑	42.74 (0.53) ↓	43.39 (0.52) ↓
FedNova [50]	27.77 (0.71) ↓	32.00 (0.64) ↓	42.62 (0.56) ↑	48.59 (0.50) ↓	58.24 (0.39) ↑
SCAFFOLD [21]	34.46 (0.64) ↑	39.26 (0.58) ↑	44.60 (0.53) ↑	55.35 (0.41) ↑	62.80 (0.34) ↑
FedNTD (Ours)	35.77 (0.64) ↑	45.47 (0.50) ↑	52.61 (0.43) ↑	60.22 (0.36) ↑	60.61 (0.34) ↑

Table 9: Accuracy@1 on CIFAR-10 (LDA $\alpha = 0.1$). The value in the parenthesis is the forgetting \mathcal{F} .

Method	IID Partition Strategy: LDA ($\alpha = 0.1$)				
	Local Epochs (E)				
	1	3	5	10	20
FedAvg [39]	29.77 (0.69)	37.70 (0.60)	46.49 (0.51)	53.80 (0.43)	57.70 (0.39)
FedProx [32]	33.37 (0.65) ↑	37.88 (0.57) ↑	47.65 (0.49) ↑	44.02 (0.50) ↓	44.98 (0.49) ↓
FedNova [50]	26.35 (0.73) ↓	24.37 (0.74) ↓	28.06 (0.71) ↓	47.41 (0.50) ↓	10.00 (Failure) ↓
SCAFFOLD [21]	13.36 (0.86) ↓	22.04 (0.75) ↓	23.12 (0.74) ↓	38.49 (0.57) ↓	47.07 (0.47) ↓
FedNTD (Ours)	33.94 (0.64) ↑	45.92 (0.50) ↑	54.42 (0.42) ↑	60.67 (0.33) ↑	62.25 (0.30) ↑

G.2 Effect of Sampling Ratio

Table 10: Accuracy@1 on CIFAR-10 (Sharding $s = 2$). The value in the parenthesis is the forgetting \mathcal{F} .

Method	IID Partition Strategy: Sharding ($s = 2$)				
	Client Sampling Ratio (R)				
	0.05	0.1	0.3	0.5	1.0
FedAvg [39]	33.06 (0.66)	40.14 (0.59)	49.99 (0.46)	52.98 (0.41)	51.48 (0.30)
FedProx [32]	35.36 (0.63) ↑	41.48 (0.57) ↑	44.54 (0.45) ↓	50.02 (0.31) ↓	52.53 (0.06) ↑
FedNova [50]	29.99 (0.69) ↓	42.62 (0.56) ↑	55.59 (0.31) ↑	56.75 (0.23) ↑	51.89 (0.34) ↑
SCAFFOLD [21]	29.15 (0.70) ↓	44.60 (0.53) ↑	55.59 (0.31) ↑	56.75 (0.23) ↑	57.88 (0.10) ↑
FedNTD (Ours)	46.99 (0.51) ↑	52.61 (0.43) ↑	59.37 (0.28) ↑	60.70 (0.18) ↑	61.53 (0.04) ↑

Table 11: Accuracy@1 on CIFAR-10 (LDA $\alpha = 0.1$). The value in the parenthesis is the forgetting \mathcal{F} .

Method	IID Partition Strategy: LDA ($\alpha = 0.1$)				
	Client Sampling Ratio (R)				
	0.05	0.1	0.3	0.5	1.0
FedAvg [39]	29.35 (0.70)	46.49 (0.51)	53.73 (0.39)	58.72 (0.25)	61.38 (0.04)
FedProx [32]	36.36 (0.63) ↑	47.65 (0.49) ↑	45.78 (0.37) ↓	49.65 (0.23) ↓	51.31 (0.07) ↓
FedNova [50]	21.31 (0.78) ↓	28.06 (0.71) ↓	45.83 (0.49) ↓	55.09 (0.50) ↓	56.79 (0.30) ↓
SCAFFOLD [21]	15.80 (0.84) ↓	23.12 (0.74) ↓	41.29 (0.51) ↓	10.00 (Failure) ↓	10.00 (Failure) ↓
FedNTD (Ours)	45.80 (0.53) ↑	54.42 (0.42) ↑	58.57 (0.33) ↑	60.88 (0.19) ↑	62.48 (0.06) ↑

H Comparison to KD

We analyze the advantage of FedNTD over KD by observing the performance of the loss function below. Note that $L(\lambda)$ moves from \mathcal{L}_{KD} to \mathcal{L}_{NTD} as λ increases, and collapses to \mathcal{L}_{KD} at $\lambda = 0$ and \mathcal{L}_{NTD} at $\lambda = 1$.

$$\mathcal{L}_{\text{KD} \rightarrow \text{NTD}} = \mathcal{L}_{\text{CE}}(q, \mathbb{1}_y) + L(\lambda), \quad (17)$$

$$L(\lambda) = (1 - \lambda) \cdot \mathcal{L}_{\text{KD}}(q_\tau^l, q_\tau^g) + \lambda \cdot \mathcal{L}_{\text{NTD}}(\tilde{q}_\tau^l, \tilde{q}_\tau^g). \quad (18)$$

The result is in [Table 12](#), which shows reaching $L(\lambda)$ to \mathcal{L}_{NTD} significantly improves the performance. This improvement supports the effect of decoupling the not-true classes and the true classes: preservation of out-local distribution knowledge using not-true class signals and acquisition of new knowledge on true classes from local datasets.

Table 12: CIFAR-10 test accuracy by varying λ .

Partition Method	KD	KD \rightarrow NTD					NTD
		0.1	0.3	0.5	0.7	0.9	
Sharding ($s = 2$)	46.2	46.4	46.9	47.6	48.8	50.2	52.6
LDA ($\alpha = 0.1$)	50.8	50.9	51.4	51.9	52.6	53.6	54.9

I Effect of FedNTD Hyperparameters

In [Figure 11](#), we plot the effect of FedNTD hyperparameters on the performance. The result shows that although FedNTD is not much sensitive to the choice of β , too small τ significantly drops the accuracy, which may be due to the too stiff not-true probability targets. The effect of both hyperparameters on the forgetting measure \mathcal{F} is in [Figure 12](#).

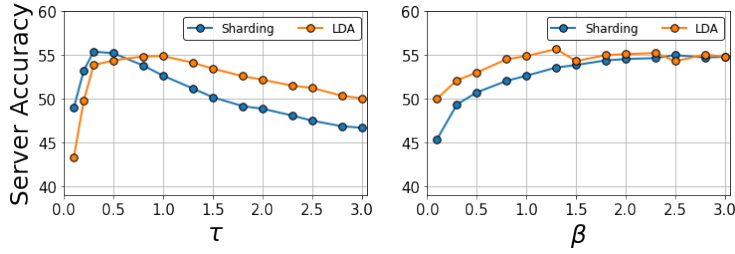


Figure 11: CIFAR-10 (Sharding: $s = 2$, LDA: $\alpha = 0.1$) test accuracy by varying FedNTD hyperparameter τ and β values.

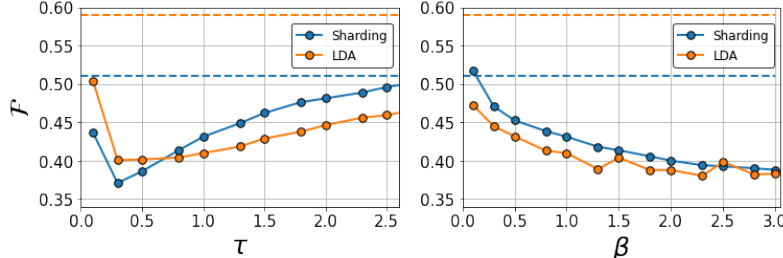


Figure 12: Forgetting \mathcal{F} of FedNTD on CIFAR-10 by varying hyperparameters. The dotted lines stands for the baseline FedAvg.

J MSE Loss for Not-True Distillation

We explore how the MSE loss on Not-True Distillation acts. In [Table 13](#), the MSE version FedNTD (FedNTD (MSE)) shows better accuracy and less forgets as β grows, but at some degree, the model diverges; thereby cannot reach the original FedNTD, which exploits softmax and KL-Divergence loss to distill the knowledge in the global model. We explain it as matching all not-true logits using MSE logits is too strict to learn the global knowledge since the dark knowledge is mainly contained in top-k logits. FedNTD controls the class signals by using temperature-softened softmax.

Table 13: CIFAR-10 (Sharding $s=2$) results by varying β for FedNTD (MSE) and FedNTD

Method	β	FedNTD (MSE)					FedNTD	
		0.0	0.001	0.005	0.01	0.05	0.1	0.3
Accuracy	40.14	40.53	42.39	43.02	44.41	44.27	Failure	52.61
Forgetting \mathcal{F}	0.59	0.58	0.56	0.55	0.53	0.53	Failure	0.43

K Visualization of Feature Alignment

To analyze feature alignment, we regard a neuron as the basic feature unit and identify individual neuron's class preference as follows:

$$\mathcal{H} = [h_1, h_2 \dots h_C], \text{ where } h_c = \sum_{i=1}^{N_c} \mathcal{O}(x_{c,i}). \quad (19)$$

Here, the $\mathcal{O}(x_{c,i})$ denotes the neuron's activation on data x_i of class c , and N_c is the number of samples for class c . For each neuron, we obtain the largest class index $\text{argmax}_i(\mathcal{H}_i)$, to identify the most dominantly encoded class semantics. A similar measure is adopted in [54]. In Figure 13, we visualize the last layer neurons' class preference. In both IID and NIID (Sharding $s = 2$) cases, the features are more well-aligned in FedNTD.

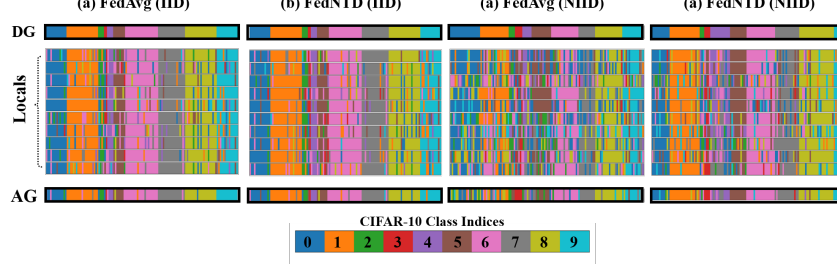


Figure 13: Visualized server test accuracy of FedAvg and FedNTD on CIFAR-10 (Sharding=2).

L Local features visualization: Hypersphere

To figure out forgetting of knowledge in the global model, we now analyze how the representation on the global distribution changes during local training. To this end, we design a straightforward experiment that shows the change of features on the unit hypersphere. More specifically, we modified the network architecture to map CIFAR-10 (Sharding $s = 2$) input data to 2-dimensional vectors and normalize them to be aligned on the unit hypersphere $S^1 = \{x \in \mathbb{R}^2 : \|x\|_2 = 1\}$. We then estimate their probability density function. The global model is learned for 100 rounds of communication on *homogeneous* locals (i.i.d. distributed) and distributed to *heterogeneous* locals with different local distributions. The result is in Figure 14

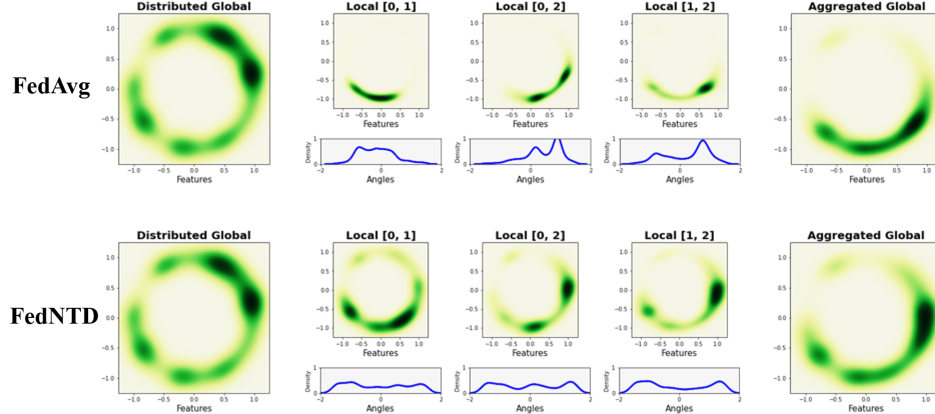


Figure 14: Features of CIFAR-10 (Sharding $s = 2$) test samples on S^2 . We plot the feature distribution with Gaussian kernel density estimation (KDE) in \mathbb{R}^2 and $\arctan(y, x)$ for each point $(x, y) \in S^1$. The distributed global model (first column) is trained on heterogeneous locals (middle 3 columns) and aggregated by parameter averaging (last column).

M Local features visualization: T-SNE

We further conduct an additional experiment on features of the trained local model. we trained the global server model for 100 communication rounds on *heterogeneous* (NIID) locals and distributed over 10 *homogeneous* (IID) locals and 10 *heterogeneous* (NIID) locals. In the homogeneous local case (Figure 15a, Figure 16a), the features are clustered by classes, regardless of which local they are learned from. On the other hand, in the heterogeneous local case (Figure 15b, Figure 16b), the features are clustered by which local distribution is learned. In Figure 17, we visualize the effect of FedNTD on the local features.

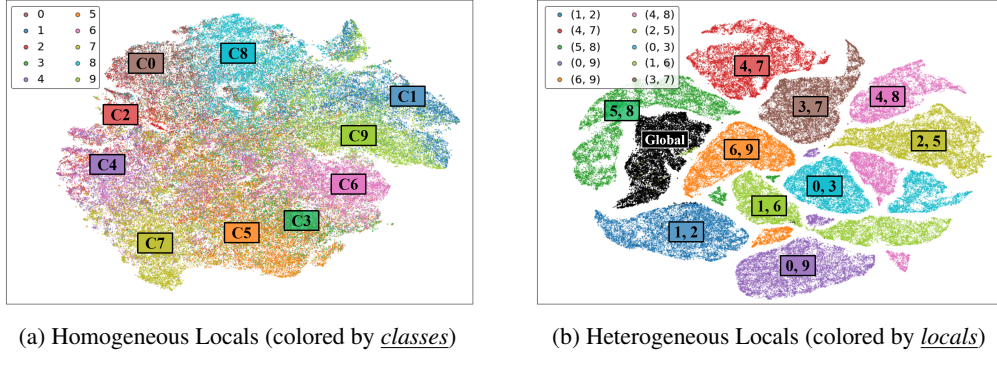


Figure 15: T-SNE visualization of features on CIFAR-10 test samples after local training on (a) *homogeneous* local distributions and (b) *heterogeneous* local distributions. The T-SNE is conducted together for the test sample features of global and 10 local models.

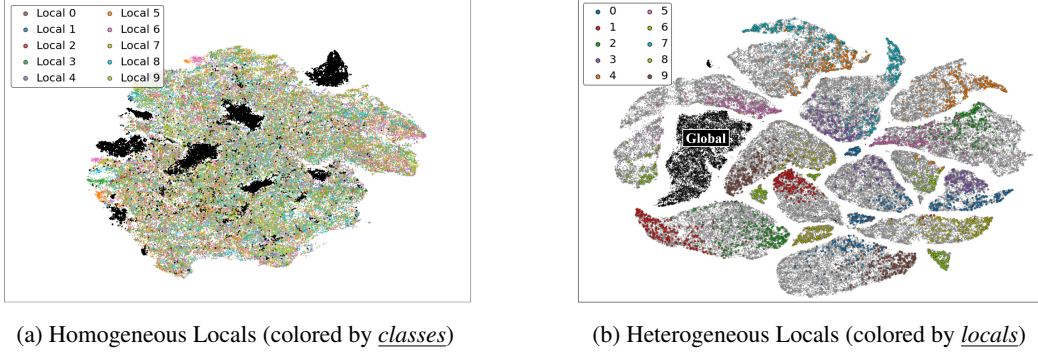


Figure 16: T-SNE visualization of feature region shifting on CIFAR-10 test samples after local training on (a) Homogeneous local distributions and (b) heterogeneous local distributions. The T-SNE is conducted together for the test sample features of global and 10 local models.

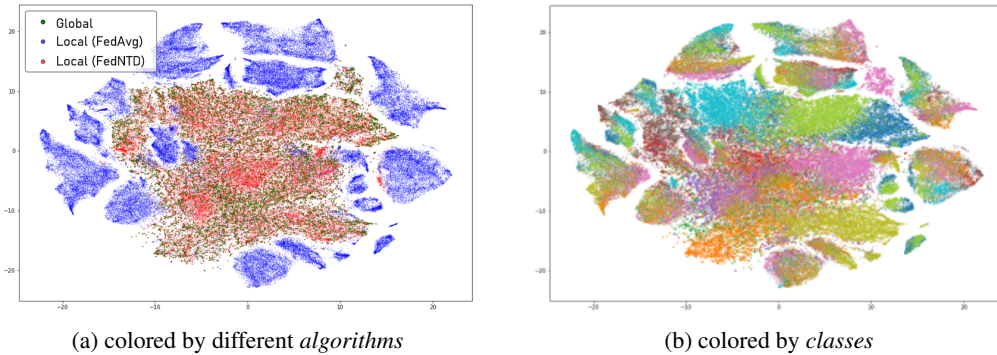


Figure 17: T-SNE on CIFAR-10 testset samples after local training on *heterogeneous* local distributions by **FedAvg** and **FedNTD**. The T-SNE is conducted together for the test sample features of global and 20 local models (10 for FedAvg and 10 for FedNTD).

N Proof of Proposition 1

Proof. Since the class-wise gradient g_i are mutually orthogonal and have uniform weight, from the unitarily invariance of the 2-norm we have:

$$\Lambda(\beta) = \frac{\frac{1}{K} \sum_{k=1}^K \|p^k + \beta \tilde{p}^k\|^2}{\|\sum_{k=1}^K p^k + \beta \tilde{p}^k\|^2} \stackrel{(\spadesuit)}{=} \frac{1}{K} \frac{\sum_{k=1}^K \sum_{c=1}^C (p^k(c) + \beta \tilde{p}^k(c))^2}{\sum_{c=1}^C (\sum_{k=1}^K p^k(c) + \beta \tilde{p}^k(c))^2} \quad (20)$$

$$\stackrel{(\clubsuit)}{=} \frac{1}{(1+\beta)^2} \frac{C}{K^3} \sum_{k=1}^K \sum_{c=1}^C (p^k(c) + \beta \tilde{p}^k(c))^2 \quad (21)$$

$$= \frac{1}{(1+\beta)^2} \frac{C}{K^3} \sum_{k=1}^K C \mathbb{E}_{c \in [C]} [(p^k + \beta \tilde{p}^k)^2] = \frac{1}{(1+\beta)^2} \frac{C^2}{K^3} \sum_{k=1}^K \mathbb{E}_{c \in [C]} [(p^k + \beta \tilde{p}^k)^2] \quad (22)$$

$$= \frac{1}{(1+\beta)^2} \frac{C^2}{K^3} \sum_{k=1}^K \left(\text{Var}_{c \in [C]} [p^k + \beta \tilde{p}^k] + (1+\beta)^2 \right) \quad (23)$$

$$= \frac{1}{(1+\beta)^2} \frac{C^2}{K^3} \sum_{k=1}^K \left(\text{Var}_{c \in [C]} \left[p^k + \beta \frac{1-p^k}{C-1} \right] \right) + \frac{C^2}{K^2} \quad (24)$$

$$= \frac{1}{(1+\beta)^2} \frac{C^2}{K^3} \sum_{k=1}^K \left(\left(1 - \frac{\beta}{C-1}\right)^2 \text{Var}_{c \in [C]} [p^k] \right) + \frac{C^2}{K^2}. \quad (25)$$

Where the (\spadesuit) follows from $p^k = \sum_{c=1}^C p^k(c) \mathbf{e}_k (\in \Delta_C)$, and (\clubsuit) holds because we are assuming uniform global data distribution. That is, we have the following equation from the symmetry over classes.

$$\sum_{k=1}^K p^k(c) = \sum_{k=1}^K \tilde{p}^k(c) = \frac{K}{C}. \quad (26)$$

By differentiating the equation (25), we have:

$$\frac{\partial \Lambda(\beta)}{\partial \beta} = \left(\frac{C^2}{K^3(C-1)^2} \sum_{k=1}^K \text{Var}_{c \in [C]} [p^k] \right) \frac{\partial}{\partial \beta} \frac{(C-(1+\beta))^2}{(1+\beta)^2} \quad (27)$$

$$= \left(\frac{C^2}{K^3(C-1)^2} \sum_{k=1}^K \text{Var}_{c \in [C]} [p^k] \right) \left(-2 \frac{C^2}{(1+\beta)^3} + 2 \frac{C}{(1+\beta)^2} \right) \quad (28)$$

$$= - \left(\frac{2C^3}{K^3(C-1)^2} \sum_{k=1}^K \text{Var}_{c \in [C]} [p^k] \right) \left(\frac{C}{(1+\beta)^3} - \frac{1}{(1+\beta)^2} \right). \quad (29)$$

By defining $M_{K,C,p} > 0$ in the first bracket, we have:

$$\frac{\partial \Lambda}{\partial \beta} = -M_{K,C,p} \left(\frac{C}{(1+\beta)^3} - \frac{1}{(1+\beta)^2} \right), \quad (30)$$

for all $\beta \geq 0$. If $\beta \leq C/2 - 1$, we have $C/(1+\beta) \geq 2$, and get following desired inequality:

$$\frac{\partial \Lambda}{\partial \beta} \leq -M_{K,C,p} \frac{1}{(1+\beta)^2}. \quad (31)$$

O Proof of Proposition 2

Proof. First, we show the first equation. The square term for the true class is:

$$\mathcal{L}_{\text{MSE}}^{\text{true}} = \frac{1}{N} \sum_{i=1}^N \sum_{c=1}^C (z_i^c - z_{i,\text{ref}}^c)^2 \quad (32)$$

Note that $\sum_{i=1}^N = \sum_{c=1}^C \sum_{i \in \mathcal{S}_c}$. By using this, we get:

$$\mathcal{L}_{\text{MSE}}^{\text{true}} = \frac{1}{N} \sum_{i=1}^N \sum_{c=y_i}^C (z_i^c - z_{i,\text{ref}}^c)^2 = \frac{1}{N} \sum_{c=1}^C \sum_{i \in \mathcal{S}_c} \sum_{c'=y_i}^C (z_i^{c'} - z_{i,\text{ref}}^{c'})^2 \quad (33)$$

$$= \frac{1}{N} \sum_{c=1}^C \sum_{i \in \mathcal{S}_c} \sum_{c'=c}^C (z_i^{c'} - z_{i,\text{ref}}^{c'})^2 = \frac{1}{N} \sum_{c=1}^C \sum_{i \in \mathcal{S}_c} (z_i^c - z_{i,\text{ref}}^c)^2 \quad (34)$$

$$= \sum_{c=1}^C p_c \left[\frac{\sum_{i \in \mathcal{S}_c} (z_i^c - z_{i,\text{ref}}^c)^2}{|\mathcal{S}_c|} \right]. \quad (35)$$

Next, we derive the not-true part of the MSE:

$$\mathcal{L}_{\text{MSE}}^{\text{not-true}} = \frac{1}{N(\mathcal{C}-1)} \sum_{i=1}^N \sum_{c' \neq y_i}^C (z_i^{c'} - z_{i,\text{ref}}^{c'})^2. \quad (36)$$

From the definition, we have:

$$\mathcal{L}_{\text{MSE}}^{\text{not-true}} = \frac{1}{N(\mathcal{C}-1)} \sum_{c=1}^C \sum_{i \in \mathcal{S}_c} \sum_{c' \neq c}^C (z_i^{c'} - z_{i,\text{ref}}^{c'})^2 = \frac{1}{N(\mathcal{C}-1)} \sum_{c=1}^C \sum_{c' \neq c} \sum_{i \in \mathcal{S}_c} (z_i^{c'} - z_{i,\text{ref}}^{c'})^2 \quad (37)$$

$$= \frac{1}{N(\mathcal{C}-1)} \sum_{c'=1}^C \sum_{c \neq c'} \sum_{i \in \mathcal{S}_c} (z_i^{c'} - z_{i,\text{ref}}^{c'})^2 = \frac{1}{N(\mathcal{C}-1)} \sum_{c=1}^C \sum_{c' \neq c} \sum_{i \in \mathcal{S}'_c} (z_i^c - z_{i,\text{ref}}^c)^2 \quad (38)$$

$$= \sum_{c=1}^C \frac{\sum_{c' \neq c} |\mathcal{S}_c|/N}{(\mathcal{C}-1)} \sum_{c' \neq c} \frac{\sum_{i \in \mathcal{S}'_c} (z_i^c - z_{i,\text{ref}}^c)^2}{\sum_{c' \neq c} |\mathcal{S}_{c'}|} \quad (39)$$

$$= \sum_{c=1}^C \tilde{p}_c \sum_{c' \neq c} \frac{\sum_{i \in \mathcal{S}'_c} (z_i^c - z_{i,\text{ref}}^c)^2}{\sum_{c' \neq c} |\mathcal{S}_{c'}|} = \sum_{c=1}^C \tilde{p}_c \frac{\sum_{i \notin \mathcal{S}_c} (z_i^c - z_{i,\text{ref}}^c)^2}{\sum_{c' \neq c} |\mathcal{S}_{c'}|}. \quad (40)$$

□

P Derivation of Equation 15

Proof. The main part of the proof is well-known inequality for smooth functions, which is derived from the Taylor approximation. Since $\mathcal{L}_i : \mathcal{W} \subset \mathbb{R}^n \rightarrow \mathbb{R}$ is smooth function, we have

$$\mathcal{L}_i(w) = \mathcal{L}_i(w_i) + \nabla \mathcal{L}_i(w_i) \cdot (w - w_i) + \int_0^1 (1-t)(w - w_i)^\top \cdot \nabla^2 \mathcal{L}_i(w_i + t(w - w_i)) \cdot (w - w_i) dt \quad (41)$$

$$= \mathcal{L}_i(w_i) + \int_0^1 (1-t)(w - w_i)^\top \cdot \nabla^2 \mathcal{L}_i(w_i + t(w - w_i)) \cdot (w - w_i) dt \quad (42)$$

$$\leq \mathcal{L}_i(w_i) + \lambda \int_0^1 (1-t)(w - w_i)^\top \cdot (w - w_i) dt \quad (\nabla^2 \mathcal{L}_i(w) \leq \lambda)$$

$$= \mathcal{L}_i(w_i) + \frac{\lambda}{2} \|w - w_i\|^2. \quad (43)$$

□

Q Proof of Proposition 3

Proof. To show this corollary, enough to show that the below minimax problem is attained on the uniform distribution.

$$\inf_{p \in \Delta_C} \sup_{\mathbb{P} \in \Pi} \mathbb{E}_{p' \sim \mathbb{P}} [\|p' - p\|]. \quad (44)$$

Let us define $p \mapsto \sup_{\mathbb{P} \in \Pi} \mathbb{E}_{p' \sim \mathbb{P}} [\|p' - p\|]$ as $F(p)$. First, we check the continuity of F . That is:

$$|F(p_2) - F(p_1)| \leq \left| \sup_{\mathbb{P} \in \Pi} \mathbb{E}_{p' \sim \mathbb{P}} [\|p' - p_2\|] - \sup_{\mathbb{P} \in \Pi} \mathbb{E}_{p' \sim \mathbb{P}} [\|p' - p_1\|] \right| \quad (45)$$

$$\leq \sup_{\mathbb{P} \in \Pi} \left| \mathbb{E}_{p' \sim \mathbb{P}} [\|p' - p_2\| - \|p' - p_1\|] \right| \leq \sup_{\mathbb{P} \in \Pi} \mathbb{E}_{p' \sim \mathbb{P}} [\|p' - p_2\| - \|p' - p_1\|] \quad (46)$$

$$\leq \sup_{\mathbb{P} \in \Pi} \mathbb{E}_{p' \sim \mathbb{P}} [\|p_1 - p_2\|] \leq \|p_1 - p_2\|. \quad (47)$$

Therefore, since the function F is 1-Lipschitz, it is clearly continuous. Now, since Δ_C is compact, we have a minimizer $p_0 \in \Delta_C$ of above minimax value. Since norm and expectation is convex function, F is convex. Therefore, for arbitrary minimizer p_0 and cycle $\sigma = (1 \ 2 \ \cdots \ C) \in \mathcal{S}_C$, we have:

$$F(\text{unif. dist}) = F\left(\frac{1}{C} \sum_i \sigma^i(p_0)\right) \leq \frac{1}{C} \sum_i F(\sigma^i(p_0)). \quad (48)$$

Now, we argue that $F(\sigma^i(p_0)) = F(p_0)$. From the definition of F ,

$$F(\sigma^i(p_0)) = \sup_{\mathbb{P} \in \Pi} \mathbb{E}_{p' \sim \mathbb{P}} [\|p' - \sigma^i(p_0)\|] = \sup_{\mathbb{P} \in \Pi} \mathbb{E}_{p' \sim \mathbb{P}} [\|\sigma^i(\sigma^{-i}(p')) - \sigma^i(p_0)\|] \quad (49)$$

$$= \sup_{\mathbb{P} \in \Pi} \mathbb{E}_{p' \sim \mathbb{P}} [\|\sigma^i(\sigma^{-i}(p')) - \sigma^i(p_0)\|] \quad (50)$$

$$= \sup_{\mathbb{P} \in \Pi} \int_{\Delta_C} \|\sigma^i(\sigma^{-i}(p')) - p_0\| d\mathbb{P}(p') \quad (51)$$

$$= \sup_{\mathbb{P} \in \Pi} \int_{\Delta_C} \|\sigma^{-i}(p') - p_0\| d\mathbb{P}(\sigma^i(\sigma^{-i}(p'))) \quad (52)$$

$$= \sup_{\mathbb{P} \in \Pi} \int_{\Delta_C} \|p'' - p_0\| d\mathbb{P}(\sigma^i(p'')) \quad (53)$$

$$= \sup_{\mathbb{P} \in \Pi} \int_{\Delta_C} \|p'' - p_0\| d\mathbb{P}(p'') = F(p_0). \quad (\Pi \text{ is } \mathcal{S}_C\text{-invariant } (\sigma^i \in \mathcal{S}_C)) \quad (54)$$

From the equation equation (48), we have:

$$F(\text{unif. dist}) \leq \frac{1}{C} \sum_i F(\sigma^i(p_0)) = \frac{1}{C} \sum_i F(p_0) = F(p_0). \quad (55)$$

Since p_0 is minimizer, we can argue that the uniform distribution also attains the minimum. \square